2021-10-26

Determining the Anthropogenic Effects on Eutrophication of Utah Lake Since European Settlement Using Multiple Geochemical Approaches

Richard Ronald Rawle Williams
Brigham Young University

Determining the Anthropogenic Effects on Eutrophication of Utah Lake Since European Settlement Using Multiple Geochemical Approaches

Richard Ronald Rawle Williams

A thesis submitted to the faculty of
Brigham Young University
in partial fulfillment of the requirements for the degree of

Master of Science

Steve Nelson, Chair
Sam Hudson
Barry Bickmore
Greg Carling

Department of Geological Sciences

Brigham Young University

ABSTRACT

Determining the Anthropogenic Effects on Eutrophication of Utah Lake Since European Settlement Using Multiple Geochemical Approaches

Richard Ronald Rawle Williams
Department of Geological Sciences, BYU
Master of Science

Recent urbanization of Utah Valley, Utah, has highlighted the impacts of anthropogenically-driven eutrophication of Utah Lake, which may lead to more frequent harmful algal blooms. To examine changes in trophic state, three freeze cores were taken from Utah Lake (Goshen Bay, Provo Bay, and near the Provo Boat Harbor) to examine the extent of eutrophication since European settlement.

^{210}Pb and ^{137}Cs chronologies were constructed for all three cores, although due to low supported ^{210}Pb in the Provo Boat Harbor core, an additional pollen analysis was performed. Lower juniper pollen counts in addition to higher POACEAE (grasses and cereals) counts above 27 cm suggests that land clearance was taking place and horizons above this depth are post-1850s, when Utah Valley was settled. Chronologies in Goshen Bay and Provo Bay show that horizons above 40 cm are post-1950s.

Hydrogen index (HI) values derived from RockEval pyrolysis were used to characterize the organic matter in the cores. Material from all three cores show an up-section increase in HI, consistent with the increasing deposition of algal matter. $\delta^{15}N_{ATM}$ and $\delta^{13}C_{VPDB}$ isotope ratios were also measured for organic matter in the cores. ^{15}N shows enrichments upward in the cores, combined with a depletion in ^{13}C across all three. $\delta^{15}N_{ATM}$ values suggest increasing anthropogenic influence with time that may contribute to algal blooms and eutrophication. $\delta^{13}C_{VPDB}$ ratios become depleted towards the top of the core showing a change in the lake's ecology which may be due to the introduction of invasive *Phragmites.*

X-Ray diffraction (XRD) analysis was used to analyze mineralogical differences. Eastern Utah Lake and Goshen Bay cores contain 70-80 % calcite, 10-15% quartz and 10% dolomite. Provo Bay samples contain 50-60% calcite, 20-30% quartz, and 10% dolomite. The dominance of calcite suggests that the sediment is dominated by endogenic minerals, albeit with a greater contribution of detrital minerals in Provo Bay. Inductively coupled plasma optical emission spectrometry (ICP-OES) was used for elemental analysis. Concentrations of phosphorous and trace metals increase in the younger sediment of all three cores, suggesting greater anthropogenic influence on lake water with time.

Overall, the rise in HI, P, trace metals, and ^{15}N since European settlement suggests that the lake has become more eutrophic and anthropogenically-impacted in the last 170 years. This highlights the importance of understanding human impacts on water quality to help mitigate any future damage to Utah Lake's ecology and waterways.

Keywords: Utah Lake, eutrophication, algal blooms, modern sediments

ACKNOWLEDGMENTS

First, I would like to express my gratitude to Dr. Stephen T. Nelson, whose patience and support allowed me to truly succeed and thrive as a graduate student at BYU. I would also like to thank Dr. Samuel M. Hudson, Dr. Gregory T. Carling, and Dr. Barry R. Bickmore for being on my thesis committee and for all of the help they have provided me.

I would also like to thank David Tingey and Kevin Rey, whose expertise in the laboratory were invaluable. Special thanks also go to Tiffany Thayne, Camille Hanocek, and Nathan Gunnell and the guidance and help they provided in completing the analyses.

My eternal gratitude also goes out to the Wasatch Water Quality Council, who provided me with the financial support to complete this study.

I also need to thank my Heavenly Father, who provided me with blessings every day. I'd like to thank my immediate family for all of their constant belief in me. Lastly, I also must thank my wife, Manon, and my daughter. Their patience, love, and support has provided me strength throughout my in graduate school.

TABLE OF CONTENTS

LIST OF TABLES

LIST OF FIGURES

1.0 Introduction

A rise in the frequency of harmful algal blooms (HABs) in lakes around the world has led many to try and understand the role that anthropogenic influences play in the eutrophication of shallow lakes (Burford et al, 2020). Specifically, the focus has shifted to show how human settlement around shallow lakes drives eutrophication and affects nutrient levels in the water (Smith and Schindler, 2009). HABs are detrimental to fish and wildlife and are also dangerous for human populations (Zanchett and Oliveira-Filho, 2013). In order to understand the influence that human populations have on the eutrophication of shallow lakes, this study examines how water quality and nutrient loads have changed with time, and to determine how differences that can be traced to human settlement play a role in affecting the water quality. This study specifically focuses on investigating Utah Lake and how European settlement since the mid-1800s has affected the lake's water quality, sediment mineralogy, deposited organic matter and nutrient sources.

Utah Lake is located in the center of Utah County, west of Provo (Fig. 1). It is the fourth largest natural lake west of the Mississippi in the contiguous United States with a surface area of 375 km^2 (Strong, 1974). Utah Lake is relatively shallow with an average depth of 2.8 meters (Brimhall and Merritt, 1981). Utah Lake is surrounded by an urban population corridor and that population has grown from 60,000 to 630,000 within the last 50 years (US Census Bureau, 2019). Utah Lake receives water from seven wastewater treatment plants (WWTP) in Utah Valley (Merritt and Miller, 2016) as well as storm water runoff from local municipalities. In the last 30 years, HABs in Utah Lake seem to have increased in frequency, and in 2019 the Utah County Health Department installed its first permanent warning signs around the lake (Spangler, 2019). A need to understand the extent of eutrophication caused by anthropogenic sources in

Utah Lake is becoming more crucial, especially as a potential for cyanotoxins released by the HABs and oxygen starvation in the water column may threaten to destroy the lake's ecosystem, including endemic endangered species such as *Chasmistes liorus*, or the June sucker. Current anthropogenic nutrient sources to the lake are well understood due to recent studies. Horns (2005) measured nutrient levels at inflows into the lake including treated inflows from anthropogenic sources and illustrated a correlation between the high nutrient levels of Utah Lake inflows being directly affected by anthropogenic sources such as WWTPs and storm water runoff. Another study (PSOMAS, 2007), produced for the Utah Division of Water Quality also determined the extent of the prevailing eutrophication of the lake along with providing more evidence of increased nutrient loads derived from anthropogenic sources. Studies have also shown that the highest levels of phosphorous are concentrated on the east side of Utah Lake, which is near the highest human population centers in Utah Valley, as well as WWTP inflows (Randall, 2019). Though current eutrophication is well documented, this study aims to extend increased nutrient loads back to the beginning of European settlement in Utah Valley and to track the water quality and sediment changes through time.

1.1 Geological Setting

Utah Lake is located west of the Wasatch Front, adjacent to an urban population corridor comprised of multiple cities (Fig. 1). The mountains in the surrounding area near Utah Lake are comprised of rocks that range from Paleoproterozoic to Triassic in age (Constenius et al, 2011). Utah Lake occupies an intermontane valley formed by extension associated with the Great Basin, which has been undergoing crustal extension for the last 17.5 Ma (e.g., Dickinson, 2006). To the east of Utah Lake lies the Wasatch fault, at the eastern boundary of the Basin and Range Province (Machete et al, 1991). Major inflows include the Spanish Fork, American Fork, and

Provo Rivers. One major outflow is the Jordan River, which flows northward to the Great Salt Lake. The other major outflow is evaporation though ~7 % of water has been estimated to exit the basin through groundwater seepage (Horns, 2005; PSOMAS, 2007). Utah Lake is a remnant of the larger Lake Bonneville system with subjacent sediment that has been deposited for the last 10,000 years. The sediment that is deposited in Utah Lake is mostly endogenic calcite and detrital quartz, though some dolomite and clays are present as well (Randall et al, 2019).

The water quality of Utah Lake obviously affects wildlife and human populations, including those living downstream, as Utah Lake and Jordan River water is used for irrigation (UDWR, 2010). It also is home to fish and wildlife species which are adversely affected by the HABs and may be negatively impacted by a decrease in oxygen levels due to further eutrophication of the lake (Landsberg, 2002: Chislock et al, 2013). Utah Lake has been designated by the State of Utah to fit a 2A and 2B criteria that designates Utah Lake as an important recreational resource which should be safe for frequent primary contact with the water, including potential ingestion, as well as being safe for infrequent primary contact, such as boating (DWQ, 2019). Boating is an important recreational activity on the lake given its proximity to a large urban population.

Worldwide, cyanotoxins have been responsible for many poisonings with some of them ending in fatalities, and constant, low-concentration exposure of cyanotoxins have also been linked to having carcinogenic effects (Zanchett and Oliveira-Filho, 2013). With increasing populations and continuous recreational exposure, understanding how anthropogenic sources have affected Utah Lake is crucial in future mitigation and keeping human and wildlife populations healthy. Utah Lake is also home to many fish species and other wildlife, including the endangered *C. liorus* (June sucker) mentioned above. Cyanotoxins from HABs have been

demonstrated to be fatal to fish and are known to bioaccumulate in organisms, including fish, in affected waters (Zamora-Barrios et al, 2019). This also poses a problem for recreational angling in Utah Lake, where fish may be ingested by human populations. As mentioned above, eutrophication also leads to decreased dissolved-oxygen levels in the water column, making anoxic water conditions that are unsuitable for most fish populations (Chislock et al 2013). As increased organic material is deposited in the lake sediment, bacterial respiration drives down the dissolved oxygen (Zhu et al, 2008).

Water from Utah Lake outflows through the Jordan River with some diversions for irrigation (https://hiddenwater.org). Though the effects of cyanotoxins on agriculture are still being investigated, Xiang et al (2019) demonstrated that microcystin, a dangerous cyanotoxin, can be absorbed into crops through irrigation with cyanotoxin-enriched waters. As eutrophication is obviously a concern in the primary productivity of nutrient-rich lakes, understanding to what extent anthropogenic eutrophication of Utah Lake has led to poorer water quality is crucial in helping mitigate future negative consequences of anthropogenic nutrient loading, which may include an increase in HAB frequency and in anoxic water conditions.

2.0 Methods

2.1 Sample Collection

Three freeze cores were collected on Utah Lake. Freeze coring was used to help limit the disruption of the laminations of watery sediment, as well as avoid sediment deformation and compaction. All three cores were obtained in August, 2019. The first core was collected west of Utah Lake State Park, near a buoy operated by the Utah Division of Water Quality (19UL-DW) and has a length of 76 cm. The second core was collected from the center of Goshen Bay (19UL-GB) and has a length of 55 cm. The third core was collected from the center of Provo Bay

(19UL-PB) and has a length of 48 cm (Table 1; Fig. 2). After the initial coring, samples were vacuum sealed in plastic sleeves and placed in a freezer at -20 °C.

2.2 Subsample Preparation

Cores were cut horizontally into approximately 1 x 1 x 5 cm cuboid subsamples and dimensions of frozen subsamples were measured using a digital caliper. Deviations from true cuboid shapes were averaged to better estimate sample volumes. Sediment from the exterior of frozen subsamples was removed by scraping subsamples with a glass slide to reduce cross contamination. The mass of each frozen subsample was recorded. Subsamples were freeze dried and then the dry sediment was reweighed.

2.3 Sediment Ages

Sediment ages were calculated using the ^{210}Pb method similar to Appleby (2002) using the constant rate of supply (CRS) model in conjunction with ^{137}Cs analysis. The CRS model was chosen due to the potential for changes in sedimentation rates, sediment resuspension and mixing, as well as non-exponential unsupported ^{210}Pb. Bulk wet and dry densities were measured and use to calculate porosity. Samples were measured at the Science Museum of Minnesota for ^{210}Pb and ^{137}Cs activities.

2.4 Rock Eval Pyrolysis

Sample pyrolysis employed a Hawk Workstation instrument, which similar to other RockEval instruments, is used primarily to determine the hydrogen index (HI) values. All subsamples from 19UL-GB and 19UL-PB were pyrolyzed and every other sample (every 2 cm) was pyrolyzed for 19UL-DW, due to the longer core (Table 2). All subsamples were analyzed using a modified methodology developed for modern sediments, as detailed in Hudson et al. (2019). This method was used to avoid incorrect interpretations due to the thermally fragile

characteristics of modern organic matter, which could change the measurements of the S1 and S2 peaks. The S1 peak represents the amount of free hydrocarbons which are released during volatilization and is used in calculating total organic carbon of the sample (Baudin et al, 2015; Peters, 1986). The S2 peak represents the hydrocarbons that are released by the cracking of kerogens during the ramped-up stage of heating during pyrolysis. Accurate and precise measurement of the S2 peak is crucial in calculating HI values.

2.5 X-Ray Diffraction

Quantitative and qualitative mineralogical analyses were done on each sample using powder X-Ray diffraction (XRD) with a Rigaku Miniflex 600 equipped with a scintillation detector and graphite monochrometer. Freeze-dried, disaggregated samples were placed in the center cavity of zero background holders. Samples were analyzed from 3-65° two-theta. XRD patterns were analyzed via the Rigaku PDXL 2 software, using the Rietveld structure refinement method (Bish and Post, 1993).

2.6 $\delta^{15}N_{ATM}$ and $\delta^{12}C_{VPDB}$

Stable isotopes $\delta^{15}N_{ATM}$ and $\delta^{12}C_{VPDB}$ of organic matter in the sediment samples were measured at the Stable Isotope Ratio Facility for Environmental Research (SIRFER) lab at the University of Utah. 300 mg of powdered subsamples were treated in 10% HCl to remove carbonates, and rinsed 4-5 times with deionized (DI) water. Samples were then placed in a Thermo Scientific SuperModulyo freeze dryer and desiccated for 48 hours. Samples were analyzed in Sn capsules at the SIRFER Lab using an isotope-ratio mass spectrometer coupled to an elemental analyzer (Johnson et al, 2018).

2.7 Elemental Analyses

Concentrations of trace metals were measured by inductively coupled plasma-optical emission spectrometry (ICP-OES). Samples were prepared similar to Yang et al (2007) to release environmentally available (adsorbed) trace metal concentrations. 400±1 mg of sediment were refluxed for one hour in Teflon beakers with 16 ml of concentrated trace metal grade HNO_3 acid. A solution of 16 ml of trace metal grade HNO_3 acid was similarly refluxed for every nine samples to provide control for sample blanks. Samples were then centrifuged and the supernatant was saved while the remaining undissolved sample was discarded. Samples were diluted 1:10 with DI water and were analyzed in a ThermoFisher iCAP 7400 Duo ICP-OES instrument. Control solutions with a known of concentration were also analyzed every nine samples to continually check for instrumental drift, to which P is especially prone.

2.8 Pollen Extraction and Pollen Counts

Pollen extraction was performed in accordance with the University of Utah's Records of Environment and Disturbance (RED) Lab's methodologies (Faegri and Iverson, 1989; Peterson, 1983). Every other subsample of 19UL-DW was chosen for pollen extraction. *Lycopodium* pollen was added to samples to act as an exotic tracer. Samples were then digested with 10% HCl. Samples were heated to 50ºC using a hot water bath in 10% KOH, and then further digested with concentrated HF. Samples were then acetolyzed using acetic anhydride and concentrated sulfuric acid for 2.0 to 2.5 minutes. Samples were placed in silicon oil and left to desiccate for 12 hours. Slides were mounted using silicon oil and analyzed with a binocular microscope at 400x magnification. At least 200 non-tracer pollen grains were counted in each sample.

3.0 Results

3.1 Chronologies Established Using ^{210}Pb, ^{137}Cs, and Pollen Counts

^{210}Pb and ^{137}Cs chronologies were constructed on cores 19UL-GB and 19UL-PB (Table 3; Fig. 3). Both cores had low supported ^{210}Pb, though when augmented with ^{137}Cs counts, relatively good chronologies were established. Samples below 35 cm in 19UL-GB were estimated to be pre-1950s. Samples below 40 cm in 19UL-PB were also estimated to have been deposited pre-1950s. 19UL-DW did not have enough supported ^{210}Pb or measurable ^{137}Cs activities to establish a chronology. As a result, the relative pollen percentages from 19UL-DW pollen counts were used to help establish a chronology. Pollen counts from 19UL-DW found a drop in the relative percentage of Juniper pollen at 29 cm depth (Fig 4). This drop in Juniper pollen most likely represents land clearance for farming from European settlers, suggesting that all samples above 29 cm represent post-European colonization (post-1850s). In addition to the pollen analysis, multiple correlations were done with geochemical changes in 19UL-DW and changes in 19UL-GB and 19UL-PB. As will be discussed later, 19UL-GB and 19UL-PB both show increases in concentration in ^{15}N, Pb, Cu, and Zn between 1935 and 1940. These increases in concentrations were correlated with the changes in concentrations at 10 cm depth of 19UL-DW and sediment above 10 cm was labeled as being deposited post-1940s. Further extrapolation of the chronology of 19UL-DW prior to 1850 was made on the assumption of a constant rate of sedimentation and should be interpreted with caution.

Pollen counts on 19UL-DW show that there is a discernable drop in the relative percentage of CUPRESSACEAE *Juniperus osteosperma* (Utah Juniper) and CYPERACEAE pollen at 29 cm (Fig. 4). AMARANTHACEAE and POACEAE relative percentages both increase at 30 cm. FAGACEAE *Quercus gambelii* (Gambel's Oak), ASTERACEAE *Artemisia*

tridentate (sagebrush) and PINACEAE pollen counts remain relatively constant throughout the core. *Typha latifolia* (Cattail), SALICACEAE, MALVACEAE, BETULACEAE, LILACAEAE, *Ephedra*, *Sambucus*, and *Sarcobatus* pollen were also present, although counts were low and remain relatively constant throughout the core.

3.2 Hydrogen Indices

For RockEval Pyrolysis, 19UL-DW has HI values that range from 10 to 86 mgHC/gTOC and shows an increase from ~1940 to present day (Fig. 5). HI values at the bottom of 19UL-GB range from 10-30 mgHC/gTOC. HI values after 1970 increase and have a maximum value around 2000, reaching 113 mgHC/gTOC. HI values after 2000 decrease, although they remain higher than the bottom of 19UL-GB (Fig 5). 19UL-PB shows much higher HI values than 19UL-DW and 19UL-GB. HI values in 19UL-PB range from 108-281 mgHC/gTOC and do not show a systematic upward increase similar to 19UL-DW and 19UL-GB, although values do seem to increase towards the top of the core post-1960 (Fig 5). All three cores were also plotted together to show HI ranges in pre-established organic matter ranges (Fig 6) (Talbot and Livingstone, 1989).

3.3 Relative Mineral Percentages

Mineralogy in 19UL-DW consists mostly of calcite, quartz, dolomite and clays, such as illite and montmorillonite (Fig. 7). Small relative percentages (~10%) of potassium (K) feldspar are present between time intervals from 1930-1950, 1760-1810, and 1650-1670. Excluding these intervals, the mineralogy was relatively consistent throughout 19UL-DW. 19UL-GB also has calcite, quartz, dolomite, and clays without discernible K-feldspar (Fig. 7). The mineralogy in 19UL-GB is relatively consistent with depth, similar to 19UL-DW (Fig. 7). 19UL-PB consists of calcite, quartz, dolomite, and montmorillonite, although it differs from the other cores by

containing small percentages of anhydrite (1.9 - 3.6%), amphibole (0.8 – 9%), albite (7.9 – 37%) and K-feldspar (5.6 – 24%) (Fig. 7). Albite is present between intervals from 2010-2015, 1980-2000, 1950-1965 and 1940-1945. Amphibole is present in the intervals of 1995-2000 and 1970-1975. K-feldspar is present from 1970-1975, 1960-1965, and 1955-1957. Anhydrite is present 2010, 1985-1990, and 1975. A calcite:quartz ratio was plotted to help determine the proportion of endogenic to detrital sediment (Fig. 8). 19UL-DW and 19UL-GB both have relatively stable ratios of calcite to quartz, while 19UL-PB has lower calcite:quartz ratios at the bottom of the core from 1950-1955 and higher ratios between 1990-2010.

3.4 Isotope Ratios for N and C

$\delta^{15}N_{ATM}$ values were relatively stable at the bottom of 19UL-DW. However, values become more enriched after 1940. $\delta^{15}N_{ATM}$ values range from 5.9 to 8.6‰ (Fig 9). $\delta^{13}C_{VPDB}$ values of 19UL-DW range from -26.0 to -27.9‰ and becomes more negative after 1940 (Fig. 10).

19UL-GB also shows an enrichment in $\delta^{15}N_{ATM}$ values towards the top of the core and values range from 5.5 to 9.3‰, although a positive shift begins after 1930 (Fig. 9). $\delta^{13}C_{VPDB}$ values of 19UL-GB range from -25.2 to -26.9‰ and do not show the same negative trend in $\delta^{13}C_{VPDB}$ values from 19UL-DW (Fig. 8). 19UL-GB has a $\delta^{13}C_{VPDB}$ maximum value which reaches its most enriched peak (-25.2‰) midway up the core around 1980. In contrast, 19UL-DW was most enriched in ^{13}C towards the bottom of the core.

$\delta^{15}N_{ATM}$ ratios in 19UL-PB range from 1.6 to 8.5‰ and also show an enrichment in $\delta^{15}N_{ATM}$ values between 1940 and the top of the core similar to 19UL-GB. 19U-3 $\delta^{13}C_{VPDB}$ values range from -24.9 to -27.9‰ and becomes more depleted after 1940. 19UL-PB shows a negative shift in $\delta^{13}C_{VPDB}$ ratios similar to 19UL-DW.

All three cores approach similar enriched values of $\delta^{15}N_{ATM}$ at the top of the core. Values range from 8 to 9‰ (Fig. 11). As for $^{13}C_{VPDB}$ ratios, both 19UL-DW and 19UL-PB reach depleted values ranging from -28 to -27‰ (Fig 12). 19UL-GB does not reach similar concentrations but the negative trend at the top of the core suggests that it may be behaving similarly to the other two cores.

3.5 Elemental and Trace Metal Concentrations

Phosphorous (P) concentrations show patterns similar to the isotope ratios (Fig. 13-14). P concentrations in the bottom of core 19UL-DW are stable at approximately 800 mg/kg. After 1900, P concentrations began to rise and reach 912 mg/kg at the top of the core with a maximum concentration of 1044 mg/kg at 2000. P concentrations in 19UL-GB begins to increase approximately after 1940 at 796 mg/kg and reaches a maximum concentration of 1113 mg/kg at the top of the core. P concentration in 19UL-PB are the highest and drastically increases after 1940, rising from 805 mg/kg to 1700 mg/kg at the top of the core with a maximum concentration of 1850 mg/kg being reached at 1985.

Lead (Pb) concentrations at the bottom of 19UL-DW are stable at an average concentration of 9 mg/kg of sediment until 1935 (Fig. 12-13). The concentration after 1935 rises to 40 mg/kg at the top of the core. Pb concentrations in 19UL-GB shows an increase during the late 1920s and the top of the core where values reach 34 mg/kg (Fig 12). 19UL-PB also shows a rise in Pb concentrations after 1940 and reaches 36 mg/kg at the top of the core. All three cores show similar concentration increases in Cu and Zn (Figures 16-20). Blank samples showed low to negligible concentrations of all trace metals, indicating that these trace-metal patterns are not affected by laboratory reagents (Table 4).

Redox sensitive trace metals, such as vanadium (V) and nickel (Ni), have concentrations that do not show the same magnitude trends as the aforementioned trace metals, having relatively stable concentrations. V concentrations range from 2 mg/kg to 12 mg/kg, and Ni ranges from 5.5 mg/kg to 12 mg/kg in all three cores (Fig. 21). V and Ni concentrations were normalized with cobalt (Co) and chromium (Cr) concentrations (Fig. 22) to plot redox states of each sample (Fig. 23). Cr concentrations range from 7 mg/kg to 17.5 mg/kg in all three cores and Co concentrations range from 1.5 mg/kg and 4.2 mg/kg (Fig. 22). Redox conditions of each sample were also plotted, indicating that all were oxic (Fig. 23)

4.0 Discussion

As human populations increase around in Utah Valley surrounding Utah Lake, the need to understand the extent nutrients from anthropogenic sources drive lake eutrophication becomes increasingly important. In addition to understanding anthropogenic impacts on Utah Lake, analysis was done to estimate the extent to which Utah Lake has been altered from its natural state, as well as potential sources for these changes.

4.1 Pollen Counts Suggest Agricultural Land Clearance at 29 cm of 19UL-DW

Due to 19UL-DW having a low unsupported ^{210}Pb and a non-measurable ^{137}Cs, pollen extraction and counting was performed to help determine its chronology. The decrease in Juniper pollen at the top of the core probably represents the clearance of native vegetation to enable farming from European colonization post-1850 (Goslar et al., 1999). The decrease in juniper pollen coincides with an increase in pollen counts from grasses and cultivated cereals (POACEAE) and agricultural weeds (AMARANTHACEAE *Chenopodium*) at 30 cm to the top of the core, which may represent increased agriculture being established following land clearance of local junipers (Fig. 4). The changes in the pollen record, which are most likely due

to anthropogenic-driven ecological impacts, suggests that samples above 30 cm represent post-1850 and changes in core chemistry above this depth occurred after European settlement in Utah Valley. This chronology suggests that the major changes seen in other chemical analyses (above 10 cm) occurred post-1940s. The pollen record of 19UL-DW also suggests that the sedimentation rate of 19UL-DW (~0.15 cm/yr) is much lower than 19UL-GB (~0.51 cm/yr) and 19UL-PB (~0.57 cm/yr).

Although some resuspension and mixing of the sediment may explain the problematic ^{210}Pb chronology for 19UL-DW (Fig. 3), the pollen record and the systematic changes in concentrations of ^{15}N, Pb, Cu, and Zn compared with the other two cores, suggest that 19UL-DW has not been grossly remixed. 19UL-DW was also collected in the deepest water (~3.5 m) compared to 19UL-GB and 19UL-PB (~1.0 m). The greater water depth of 19UL-DW also suggests that it is least susceptible to resuspension and mixing (Dusini et al, 2009).

4.2 Increasing Algal Input in Deposited Organic Matter May Indicate Rising HAB Frequency

Increasing HI values in all three cores illustrates changes in the types of organic matter being deposited in the lake sediment (Fig. 5). The increase in HI in 19UL-DW is consistent with an increasing algal component in the organic matter (Fig. 6). Algae have higher HIs as they containing more saturated compounds and less cellulose than vascular plants (Talbot and Lærdal, 2000; Talbot and Livingstone, 1989). Cellulose contains abundant OH groups that decrease the relative proportion of H in organic matter. Although the HI values are well within the overall range for terrestrial plants, the rise in HI toward the top of the core may suggest higher proportions of algae were added to the total organic matter budget. The increase in apparent algal input took place at the beginning of the 1950s, and may record an increasing algal bloom frequency.

19UL-GB also shows a positive increase in HI values, with the change beginning after 1950, though values begin to drop after 2000 (Fig. 5). The positive shift of HI values in the lower half of the core suggests that the organic matter is being enriched in algal sources, similar to 19UL-DW (Fig. 6) (Talbot and Lærdal, 2000). The negative trend in the top of the core may represent recent changes in nutrient loads coming from differences in modern farming practices (Tong and Naramngam, 2007).

19UL-PB has HI values that lie in the terrestrial plant range and the mixed algal/terrestrial plant range and are higher overall than 19UL-DW and 19UL-GB(Fig. 6), indicating that algae have always been an important component of organic matter in Provo Bay. Although the positive trend in the upper core is not as distinctive as in the others, it is present between from 1950 and the top of the core and can be resolved using a three-point moving average (Fig. 24). The lack of an easily discernable positive trend, similar to 19UL-DW and 19UL-GB, may be caused by abundant emergent vegetation that grows in Provo Bay, buffering changes in the algal of the organic matter. Nonetheless, the overall higher HI values in 19UL-PB may also be explained by a higher overall proportion of algae in the organic fraction of sediment.

4.3 Mineralogy Shows Alkaline Lake with some Detrital Deposition

The overall mineralogy of 19UL-DW reflects a shallow, alkaline lake. Though some of the calcite that is present in the core may be detrital, it is likely that most of the calcite is endogenic due to the high pH of Utah Lake coupled with high concentrations of dissolved calcium and bicarbonate in the water (Fig. 7) (Horns, 2005). The quartz, dolomite, montmorillonite, illite and K-feldspars present in 19UL-DW are likely mostly detrital from nearby sedimentary and altered volcanic units (Brimhall and Merritt, 1981). The mineralogy of 19UL-DW has not changed much through time and the occurrence of K-feldspar most likely

represents flooding or storm events where minerals were transported more effectively to the site of deposition. One possible source for the K-feldspars is Dry Creek (Fig. 1) which drains the Little Cottonwood Stock to the north of Utah Lake (Biek, 2005).

Mineralogy of 19UL-GB was similar to 19UL-DW (Fig 8), giving further evidence of the high alkalinity of the lake. One difference is a lack of K-feldspar, which may be due to Goshen Bay being out of the depositional influence of Dry Creek, (Fig. 7) (Biek, 2005). The weight percentages of mineral components stay roughly consistent throughout the core except for several horizons containing elevated percentages of illite and montmorillonite. These horizons may represent events where detrital deposition was higher due to increased runoff into the lake. Despite these horizons, the mineralogy reflects deposition that is mostly endogenic processess.

The mineralogy of 19UL-PB differs from the other cores as the relative percentage of calcite in the sediment is much lower while quartz is higher (Fig. 7). 19UL-PB also contains other detrital minerals such as albite, amphibole, and K-feldspar in the lower middle section of the core. The lower calcite composition coupled with the relative increase of quartz (Fig. 8) and the other detrital minerals suggests that deposition of sediment in Provo Bay is much more dependent on allochthonous processes, especially from 1950 to 1995 (Fig. 7). Detrital minerals (amphibole, K-feldspar, and albite) in 19UL-PB may be derived from the Santaquin Complex (Nelson et al. 2002), which may have drained into Utah Lake from alluvial deposits from the south (Clark, 2009; Solomon, 2010). A fraction of the minerals may also have been derived from the Moroni formation which is drained by the Spanish Fork River (Constenius, 2011). Calcite composition increases moving up the core especially from 1950 to the present. The increasing calcite deposition towards the top of the core may be related to rising pH of Provo Bay, as an increased algal presence sequesters more CO_2, which in turn would raise the pH, decreasing the

solubility of Ca (Heath et al, 1995). The higher calcite percentages also show a shift where endogenic deposition overtakes detrital deposition. Overall, 19UL-PB shows that Provo Bay has been historically more influenced by detrital sediment deposition although that has changed the last 30 years.

4.4 Nitrogen Isotopes Suggest Increasing Anthropogenic Input

All three cores show increased concentrations of ^{15}N deposition since the 1940s (Fig. 9, 11). The positive shifts in the $\delta^{15}N_{ATM}$ values across all three cores show that nutrients being added to the lake are being derived from a higher trophic source in the last 80 years (Fig 9) (Wada, 2009). In anthropogenically-impacted systems, these higher trophic sources most likely include treated wastewater, septic effluent, or agricultural runoff as discussed below. The $\delta^{15}N_{ATM}$ values near the top of the core generally exceed those of pristine aquatic systems.

All $\delta^{15}N_{ATM}$ values begin to stabilize toward the top of the cores between 8-9‰ (Fig. 11). Previous studies have found that wastewater effluent has $\delta^{15}N_{ATM}$ values in the range of 4.3-17.4‰ with a median value of 10.8‰, and cow manure $\delta^{15}N_{ATM}$ values that range from 10-24‰ (Aravena et al, 1993; Widory et al, 2004). The $\delta^{15}N_{ATM}$ values in all three cores are well within the effluent $\delta^{15}N_{ATM}$ range and are near the lower range of cow manure. The increase in $\delta^{15}N_{ATM}$ ratios in the Utah Lake cores most likely represents an increase in nutrients from anthropogenically influenced discharge (AID), such as treated wastewater, feedlot and storm water runoff. The increasing ^{15}N concentrations coupled with the increase in HI values, also correlate to increased human populations in Utah Valley (Fig 25). Thus, the rise in algal blooms is likely driven by exogenous AID (Gilbert et al, 2018) and greater algal input into the sediment budget of the lake (Fig 6).

4.5 Carbon Isotopes Reflect Changes in the Lake's Ecology

$\delta\,^{13}C_{PDB}$ values from all three cores range from -27.9 to -24.5‰, well within C3 plant ranges, which suggests the bulk of the organic matter originates from C3 sources (Fig. 10, 12) (Clark and Fritz, 1997). The rise in ^{13}C concentrations, however, throughout the cores are most likely due to changes in the lake's ecology. Though some studies have linked depleted ^{13}C to oligotrophic conditions (Brenner et al. 1999), the changes in ^{13}C for Utah Lake is most likely due ecological differences in the ^{13}C content of dominant species in Utah Lake. One such source for the rising ^{13}C may be the expansion of *Phragmites australis,* which has a measured $\delta^{13}C_{PDB}$ between -27 and -28‰ (Choi et al, 2005 and Gichuki et al, 2001), which is at the low end of the range of measured $\delta\,^{13}C_{PDB}$ of organic matter. *Phragmites* was introduced to Utah waterways around 150 years ago (Chambers et al, 1999) and has continued to expand. Thus, *Phragmites* may be responsible for lower $\delta^{13}C_{PDB}$ near the top of the cores. *Phragmites* may not be the sole cause, but it illustrates that changes in organic matter ^{13}C may reflect changes in lake ecology driven by anthropogenic influences, even if changing plant communities are all within the C3 photosynthetic pathway.

4.6 Elevated Phosphorous Loading may be Derived from AID

The relatively high concentrations of P in sediment pre-1900s are likely originating from the nearby geologic formations rich in phosphates that are drained into Utah Lake, such as the Phosphoria Formation, which is partially drained by the Provo River (Hein et al, 2004). Other sources for natural phosphates also include the multiple limestone geologic units that surround Utah Valley (McGlathery et al, 1994 and Constenius et al, 2011). The rise of P concentrations from background values in all three cores, starting in the early 1900s, is probably best explained by increased nutrient loading from AID (Jarvie et al, 2006). The rise in P in all three cores

coincides with the increase in population growth (and accompanying wastewater discharges) in Utah Valley (Fig. 14, 25) beginning around the 1950s. The high P concentrations in Provo Bay may be due to the Provo WWTP, which discharges treated effluent into Provo Bay and may not mix as efficiently with the rest of the lake (Bradshaw et al, 1976). The stabilization of P levels after 1960 may be due to the sediment reaching its maximum P adsorption capacity, although further research would need to be done to find the maximum adsorption (Zhang et al, 2015). It could also be due to improved P removal from AID as populations grew. The earlier shift to higher concentrations of P after 1880 in 19UL-DW, which is near the Provo River Delta, most likely is due to anthropogenic influenced discharge from the nearby early Provo settlement that was founded next to the Provo River, which was settled in 1849 (Table 5) (Moffitt, 1975).

4.7 Trace Metals Trends Used as an Indicator of European Settlement Surrounding Utah Lake

The increase of heavy metals concentrations in all three cores also corresponds with the aforementioned rising P concentrations. The rise of Pb, Cu, and Zn concentrations started between 1920 and 1960 (Fig. 26, 27, and 28) and they continue to rise to the present. Similar to other anthropogenic impact studies of freshwater lakes (Romano et al., 2018; Smith et al., 2008), the increase in Pb, Cu, and Zn concentrations at ~1950 in 19UL-DW most likely represents heavy metals being introduced to Utah Lake from industrial sources. Likely trace metal sources may include steel and coke production at Geneva Steel, which was built in 1944 (Roper, 1994). The earlier increasing concentration of Pb, Cu, and Zn in the 1920s in 19UL-GB and 19UL-PB are likely also influenced by the Columbia Ironton Plant, which was located several miles southeast of Provo Bay (Moffit, 1975), and the Tintic Standard Refinement Mill, which was built south of Goshen Bay (James, 1984). Both were built in the early 1920s, making them likely candidates for the increases in heavy metals in Provo and Goshen Bays prior to the completion of

Geneva Steel. The later shift in heavy metal concentrations present in 19UL-GB around 1970 is most likely due to continued heavy metal input from industrial effluent from Geneva Steel, as well as continued contributions from the Columbia Ironton Plant and from growing commercial and municipal activities around the area (Chaterjee et al, 2006).

Other contributors to the Pb concentration growth in the sediment may be due to factors such as the use of tetraethyllead (TEL) as component in gasoline (Siver and Wozniak, 2000), which started in the early 1920s (Table 5) (Seyferth, 2003). However, there is no decrease in Pb concentrations due to the discontinuation of the wide use of TEL after the 1970s, such as observed by Silver and Wozniak (2000) in Crystal Lake, Connecticut. Although there is no apparent decrease in Pb, TEL clearly added some Pb to Utah Lake through atmospheric fallout from automobile exhaust (Siver and Wozniak, 2003 and Chaterjee et al, 2006).

Major mining and steel production has been discontinued around Utah Lake, with the last being Geneva Steel closing in 2002 (Table 5). The concentrations of heavy metals in the lake still seem to be rising or remaining consistently higher than previous background levels. These higher concentrations may be compensated by other sources that are linked to the growing population surrounding Utah Lake, such as increased road runoff (Rice et al, 2002; Legret and Pagotto, 1999), heavy metals in treated sewage effluent (Wang et al, 2005), and runoff from other municipal and urban areas (Gnecco et al, 2005). Although the mass flux of these anthropogenic sources has not been measured in Utah Valley, they are most likely an additional source to the higher concentrations of heavy metal in Utah Lake.

4.8 Redox Sensitive Trace Metals and Oxic Condition of Sediment Suggest Lake is Well-Mixed

Redox sensitive V and Ni concentrations show similar increasing trends towards the top of the cores, however they are much less pronounced then Pb, Cu, and Zn concentrations (Fig.

21). The increasing V and Ni concentrations are most likely derived from fossil fuel combustion (Hope, 1997) and metal production facilities (Poznanović Spahić et al, 2018) and not from increasing anoxic conditions in the lake (Huang et al, 2015). Co and Cr concentrations also have increasing concentrations post-1950s which may also be due to increased steel production from Geneva steel and the Columbia Ironton Plant (Poznanović Spahić et al, 2018) (Fig. 22).

The oxic redox-state of the sediment suggests that Utah Lake is well mixed on average (Riquier et al, 2005) (Fig. 23). The oxic conditions may be a result of the shallow nature of the lake which is mixed by wave action (Shaw et al, 2004). The oxic state of the lake also suggests that any anoxia that is driven by episodic eutrophication, and excessive primary production may be insignificant when compared to the dissolved oxygen added by wave action and mixing in the shallow waters of Utah Lake.

5.0 Summary and Conclusions

With the beginning of European settlement in the early 1850s, Utah Lake has been surrounded by exponential population growth, especially after 1950. Understanding how settlement causes changes in the lake is crucial in mitigating negative impacts, such as HABs, and eutrophication caused by anthropogenic sources. The results suggest that Utah Lake has become more eutrophic since European settlement the increase is most likely due to anthropogenic sources. Though the redox conditions of the lake have not changed overall, evidence of anthropogenically-driven eutrophication was found in simultaneous rising HI indices, enrichment of ^{15}N isotopes, increasing sediment P concentrations, and rising sediment concentrations of heavy metals, such as Pb, Cu, and Zn. All of these nutrient and trace-metal shifts coincide with a rising population in Utah Valley and in industrially activity, suggesting that the eutrophication present in the lake has increased due to AID. The implication for this

study suggests that the health of Utah Lake, and other eutrophic lakes, may be improved by enacting measures that decrease nutrient and metal discharges as populations rise.

6.0 Tables

Table 1. UTM Coordinates for Freeze Core Collection Sites

Core ID	UTM Coordinates (UTM NAD83. Zone 12T)
19UL-DW (Deep Water Near Buoy)	435095E, 4454408N
19UL-GB (Goshen Bay)	425667E, 4440198N
19UL-PB (Provo Bay)	440472E, 4449007N

Table 2. Spacing of Samples Analyzed per Core

Core ID	Core Length (cm)	Pyrolysis	Mineralogy	$\delta^{15}N$ and $\delta^{13}C$	ICP-OES	Pollen
19UL-DW	76	EO	A	EO	A	EO
19UL-GB	56	A	A	EO	A	N/A
19UL-PB	48	A	A	EO	A	N/A

Note: "A" denotes cores that had every subsample analyzed. "EO" represents cores that every other cm depth was analyzed. N/A represents analyses that were not applicable to specific cores.

Table 3. ^{210}Pb and ^{137}Cs activities for Utah Lake Cores

Core ID	Depth (cm)	^{210}Pb (total) (pCi/g)	^{214}Pb (pCi/g)	^{137}Cs (pCi/g)
19UL-GB	5-6	1.75	0.52	0.28
19UL-GB	11-12	1.18	0.81	0.22
19UL-GB	17-18	1.13	0.76	0.40
19UL-GB	23-24	1.02	0.69	0.28
19UL-GB	29-30	0.59	0.50	0.06
19UL-GB	37-38	**	**	trace
19UL-PB	5-6	1.04	0.28	0.25
19UL-PB	11-12	1.04	0.62	0.37
19UL-PB	17-18	1.00	0.79	0.27
19UL-PB	23-24	1.12	0.53	0.24
19UL-PB	29-30	0.67	0.22	0.25
19UL-PB	35-36	**	**	0.18
19UL-PB	43-44	**	**	0.00
19UL-DW	1-2	**	**	trace
19UL-DW	5-6	1.09	0.68	0.00
19UL-DW	11-12	1.20	0.71	0.00
19UL-DW	17-18	2.10	1.32	0.00
19UL-DW	23-24	0.53	1.01	0.00
19UL-DW	29-30	0.79	0.78	0.00

Table 4. ICP-OES Results for Blank Samples

Blank ID	P (mg/kg)	Pb (mg/kg)	Cu (mg/kg)	Zn (mg/kg)
1	0.5	0.0	2.6	2.0
2	0.0	0.3	0.8	2.4
3	0.0	0.4	0.0	3.0
4	0.0	0.3	3.2	5.0
5	0.2	0.0	1.1	2.4
6	0.5	0.0	0.2	3.3
7	0.0	0.2	1.4	2.4
8	0.0	0.0	1.3	1.1
9	0.0	0.2	1.0	1.6
10	0.7	0.4	1.0	1.7
11	0.0	0.0	0.0	1.6
12	0.0	0.0	0.0	1.2
13	0.0	0.0	0.0	1.5
14	0.0	0.0	0.0	1.6
15	0.9	0.0	1.1	1.6
16	0.7	0.0	1.3	1.2
17	0.4	0.0	0.0	1.7
18	0.3	0.0	0.5	1.3
19	0.0	0.0	0.0	1.8
20	0.0	0.0	0.0	1.4

Table 5. Utah County Historical Events/Activities

Year	Description of event/activity
2002	Geneva Steel ceases operations
1970s	TEL stops being added to gasoline
1958	Orem Wastewater Treatment Plant is completed and begins operations
1950-1955	Provo Wastewater Treatment Plant is completed and begins operations
1944	Construction finished on Geneva Steel
1923-1929	Construction of Columbia Ironton Plant
1920-1923	Construction and operation of the Tintic Standard Reduction Mill
1920s	TEL begins to be widely used as antiknock agent in gasoline
1870-1880	Introduction of invasive *Phragmities australis* into Utah's waterways
1870	Mining begins in the Tintic Mountains
1849	Onset of European settlement of the Provo area

7.0 Figures

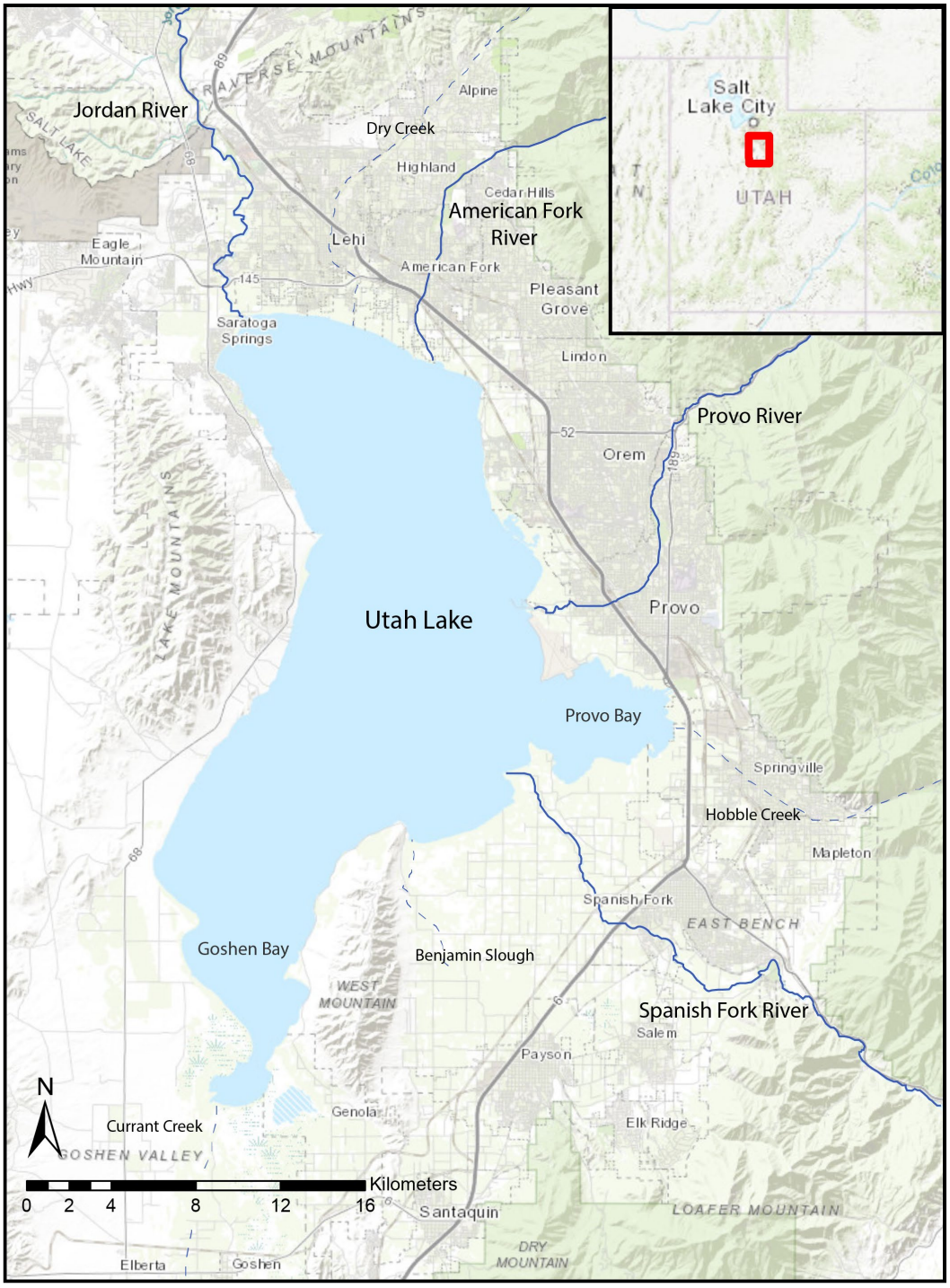

Figure 1. Map of Utah Lake within Utah Valley, Utah. The lake is bound by the Wasatch Mountains (to the east) and Lake Mountains (to the west). Most major urban areas lie on the north and east side of Utah Lake

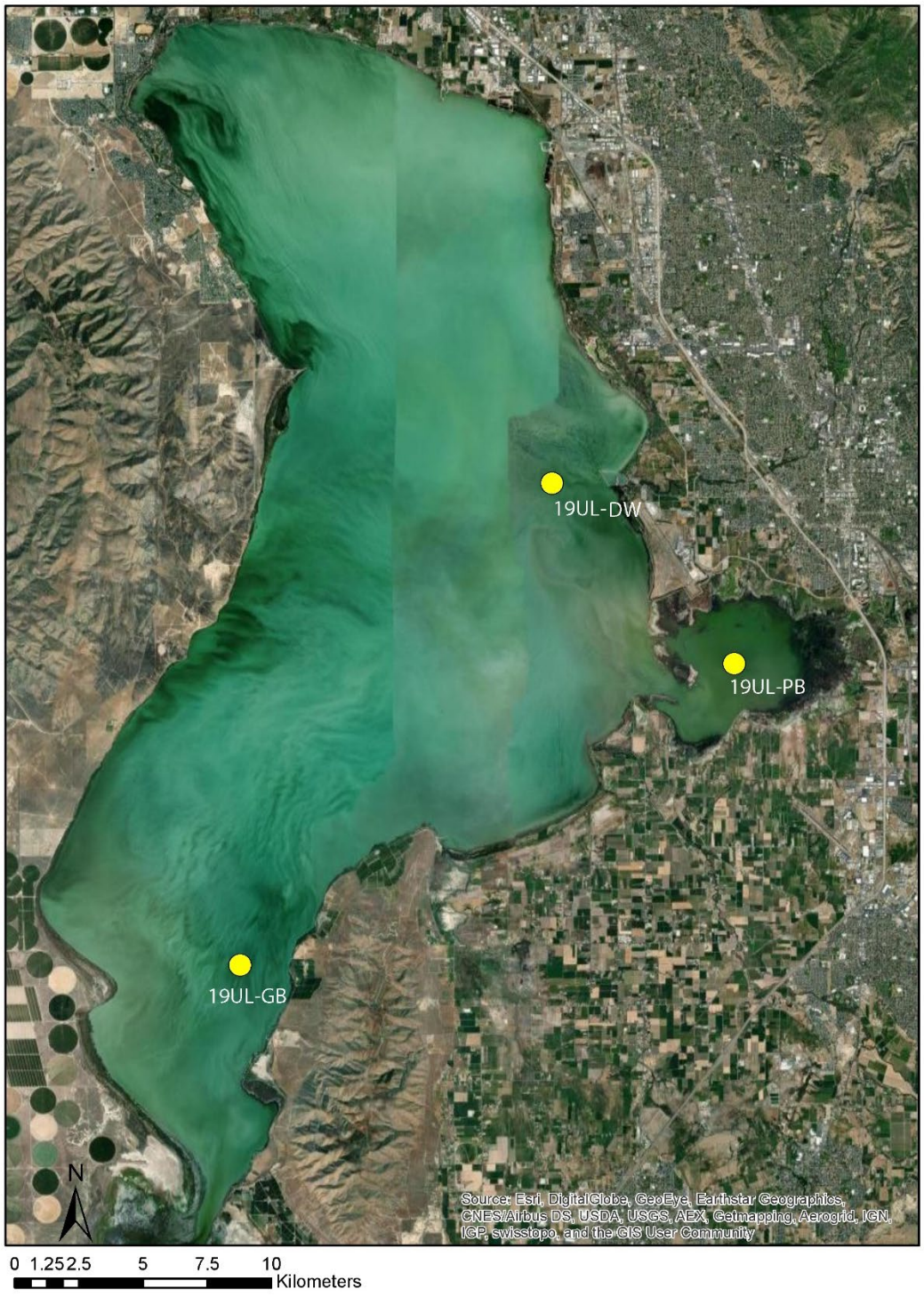

Figure 2. Map of Utah Lake Core Sample Locations. Cores were taken from the Provo and Goshen bay to understand how nutrients from these locations differ from the rest of Utah Lake.

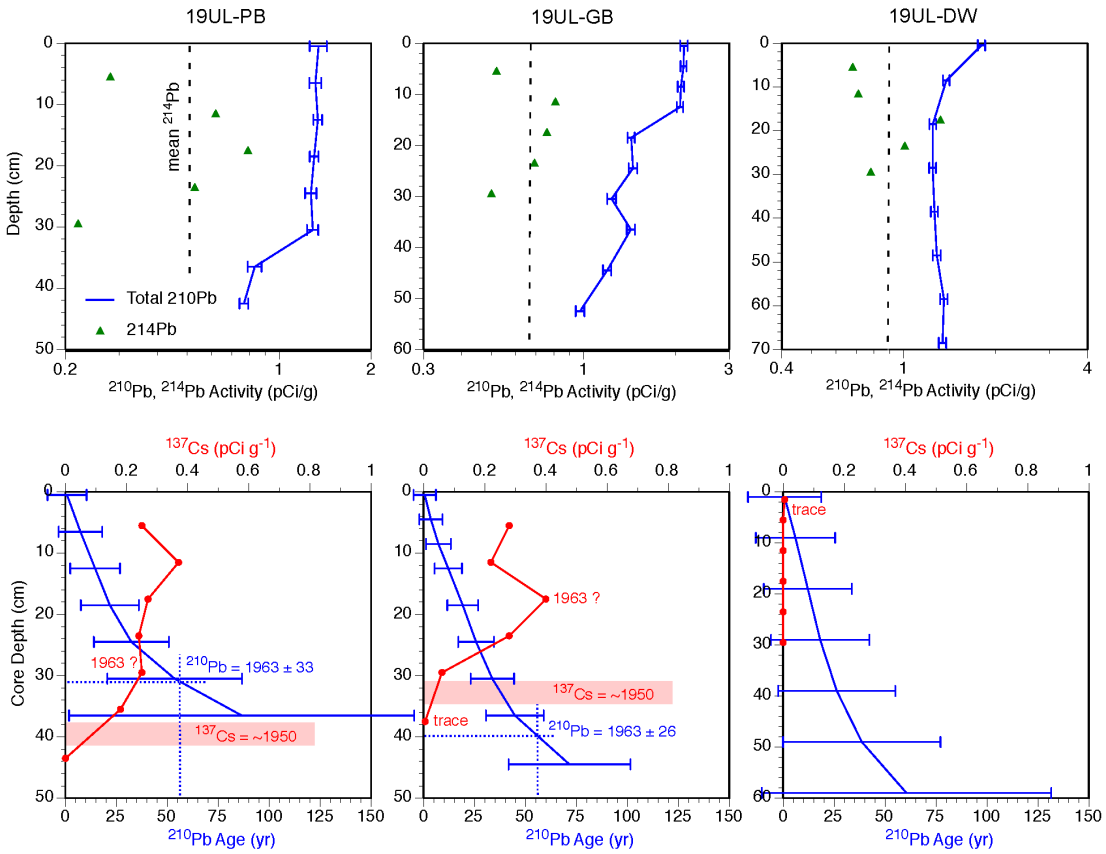

Figure 3. ^{210}Pb and ^{137}Cs counts provided by the Science Museum of Minnesota ^{210}Pb Lab. ^{210}Pb activities were low in all cores. ^{137}Cs activities were measurable in 19UL-GB and 19UL-PB. Due to the lack of high ^{210}Pb activities and ^{137}Cs activities in 19UL-DW, a pollen analysis was necessary to help determine chronology.

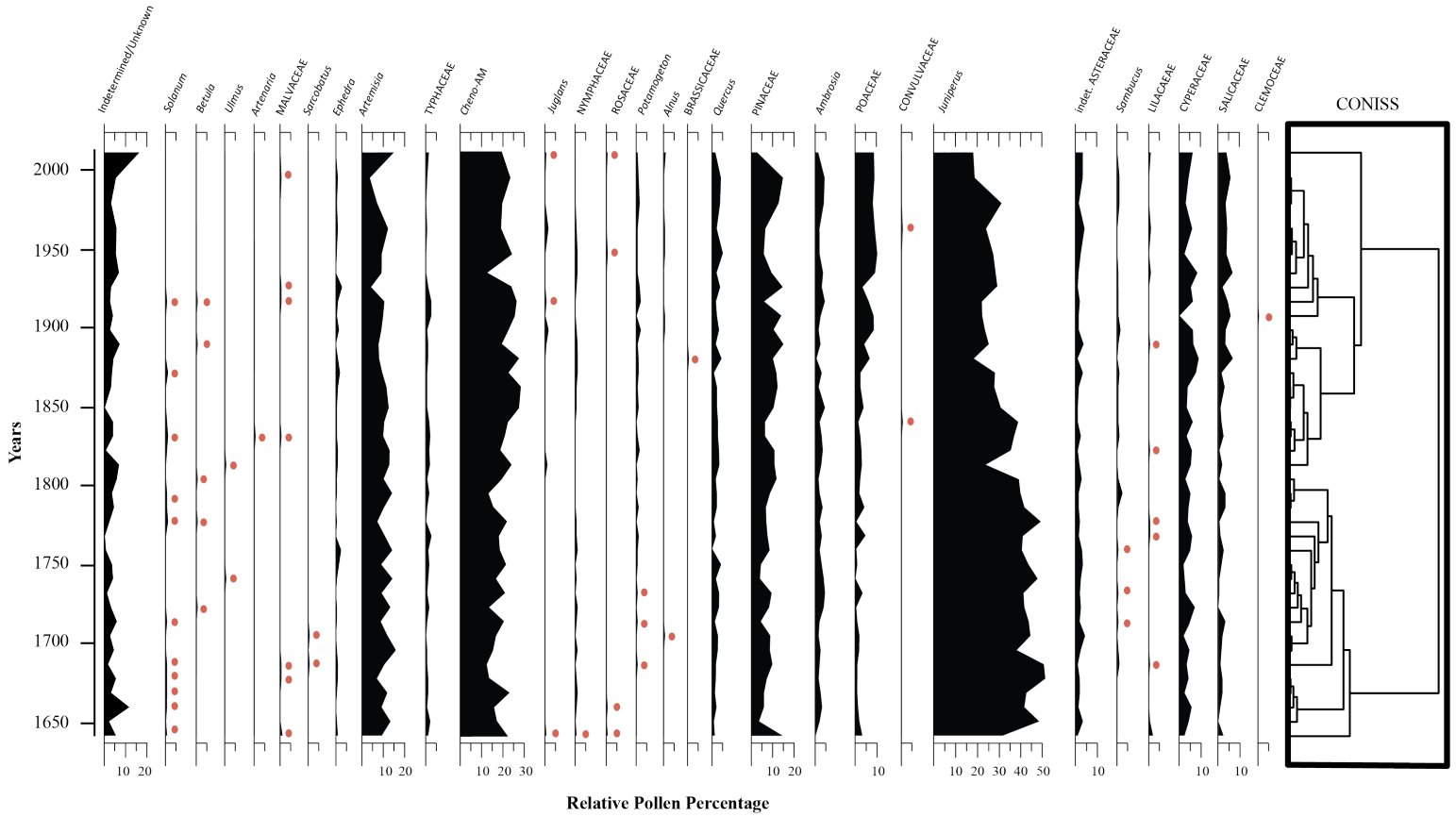

Figure 4. Relative Pollen Percentages of 19UL-DW. Pollen was identified to its lowest possible taxonomic group. Note that low relative pollen percentages were marked with a red circle to help better identify small changes. *Juniperus* stays relatively constant until it drops around 1850 and remains at a lower percentage to the top of the core. POACEAE and *Cheno*-AMs both increase post 1850. PINACEAE and *Artemisia* stays relatively constant through the core. The drop in *Juniperus* and the subsequent rise in POACEAE may represent land clearance for farming as European settlers moved in in 1850.

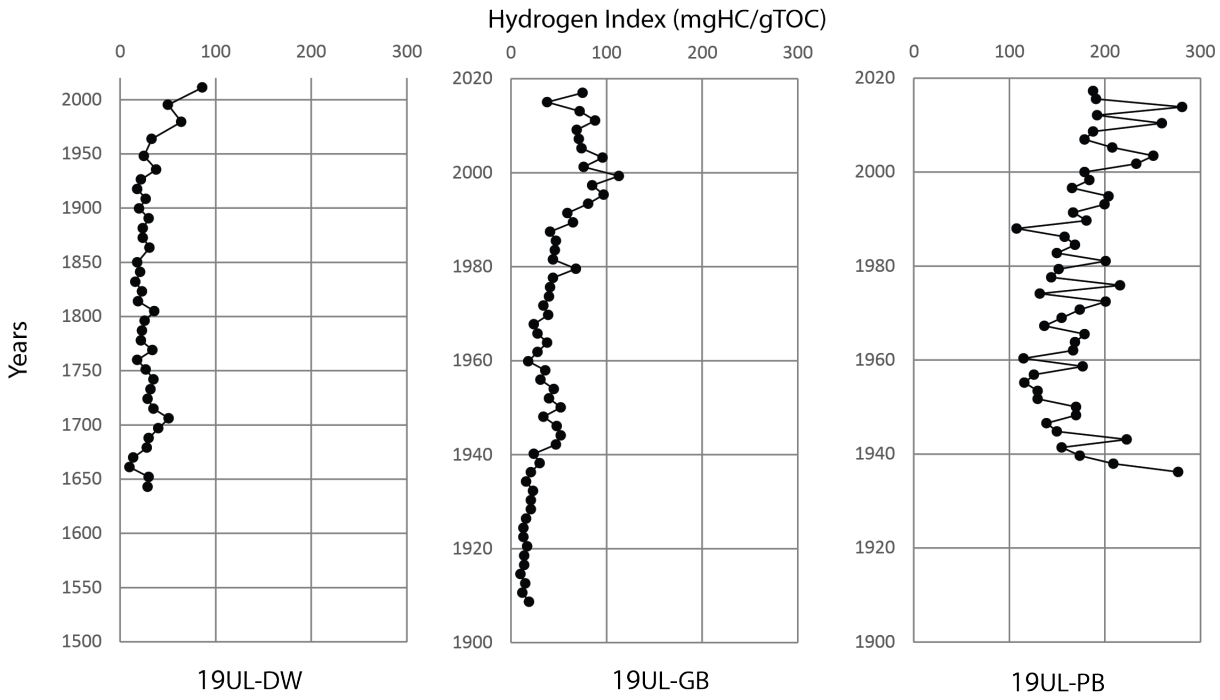

Figure 4. Hydrogen Indices of Utah Lake Cores. 19UL-PB has the highest values which may be due the high amounts of emergent vegetation in Provo Bay (Talbot and Livingstone, 1989). While all HI values are within the range of terrestrial plants, an increase in algal organic matter may drive up the HI values of the overall organic matter budget.

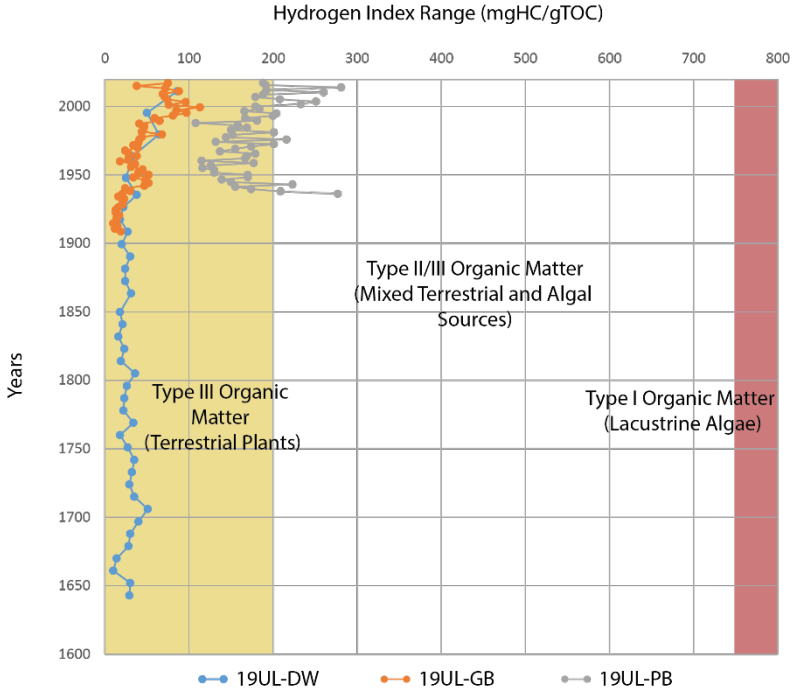

Figure 6. HI indices plotted on HI organic matter range. Both 19UL-DW and 19UL-GB are in the terrestrial plant range, while 19UL-PB is in the boundary of terrestrial plant matter and the mixed terrestrial plant and algal sources.

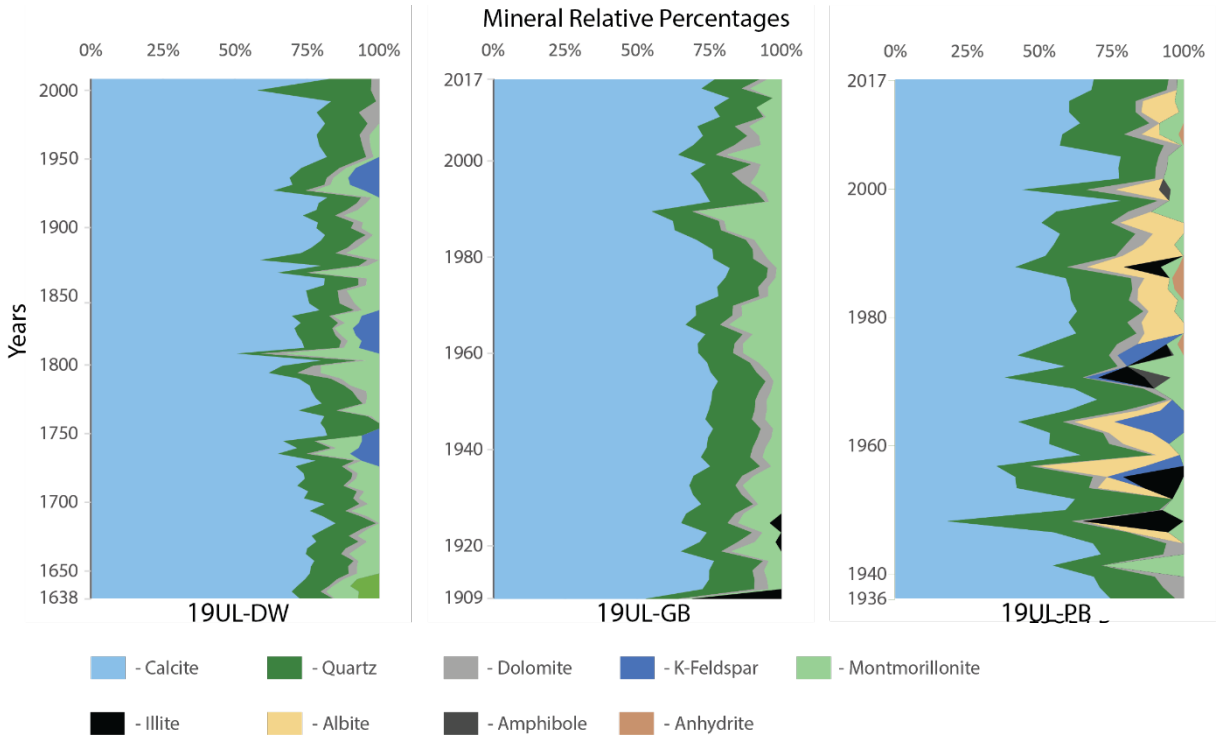

Figure 7. Mineralogy of Utah Lake Cores. While 19UL-DW and 19UL-GB have similar mineralogies, (calcite, quartz, dolomite and clay) 19UL-PB contains more detrital minerals. Calcite precipitation seems to also increase towards the top of the core of 19UL-PB.

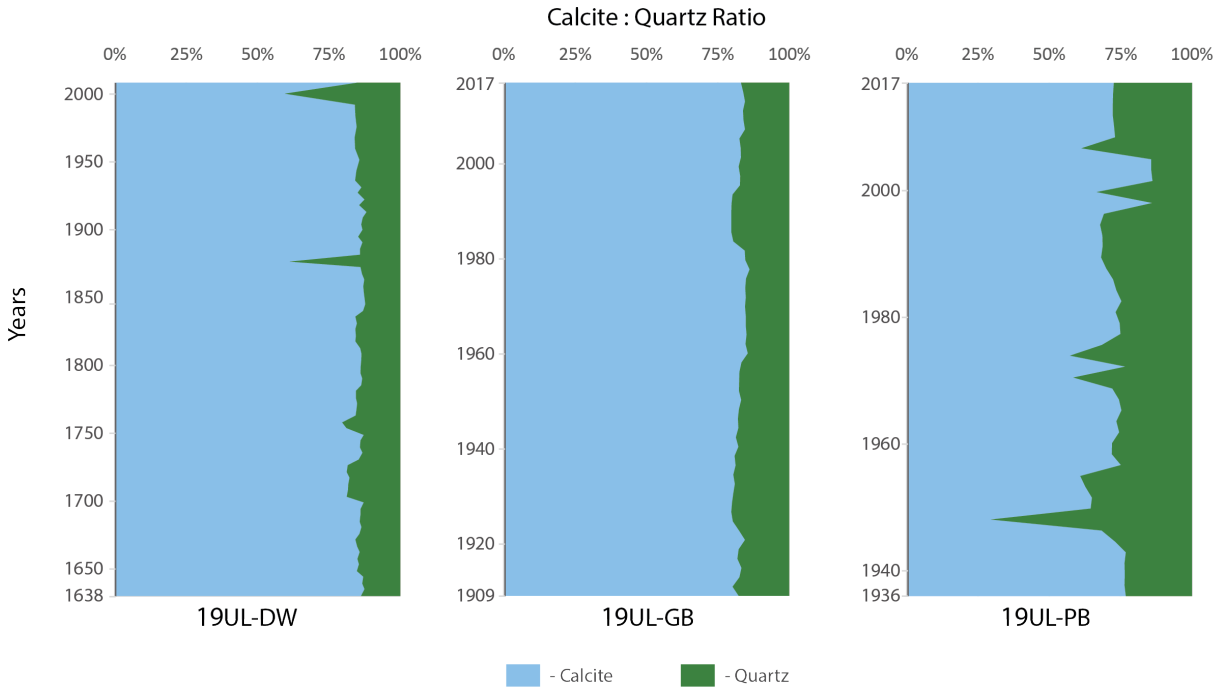

Figure 8. Calcite:Quartz ratio of Utah Lake cores sediment. 19UL-DW and 19UL-GB both have relatively stable ratios showing the lake is very alkaline. 19UL-PB also stays stable though it does seem to have higher ratios further up the core, suggesting that the pH of Provo Bay has risen compared to past values.

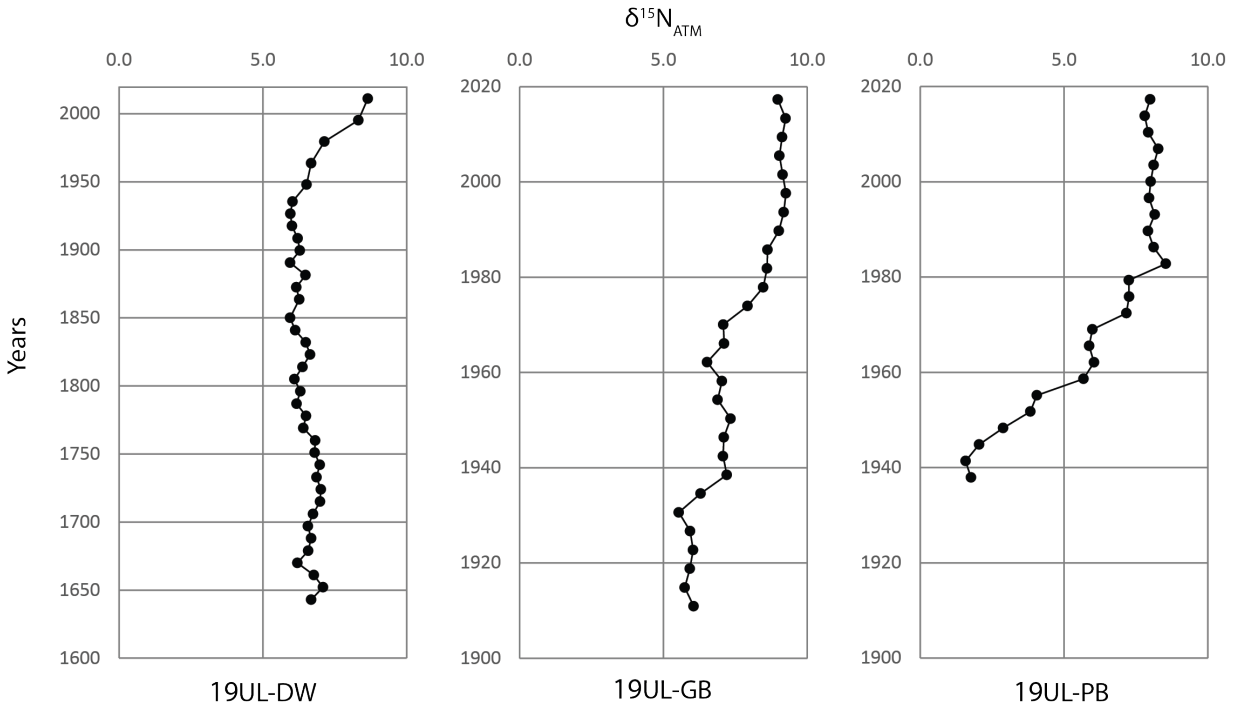

Figure 9. $\delta^{15}N$ values of organic matter of Utah Lake cores. All cores have positive shift in $\delta^{15}N$ values which begins around 1940. This positive deflection may represent nutrients coming from sources on a higher trophic level than was previously entering the lake (Wada, 2009).

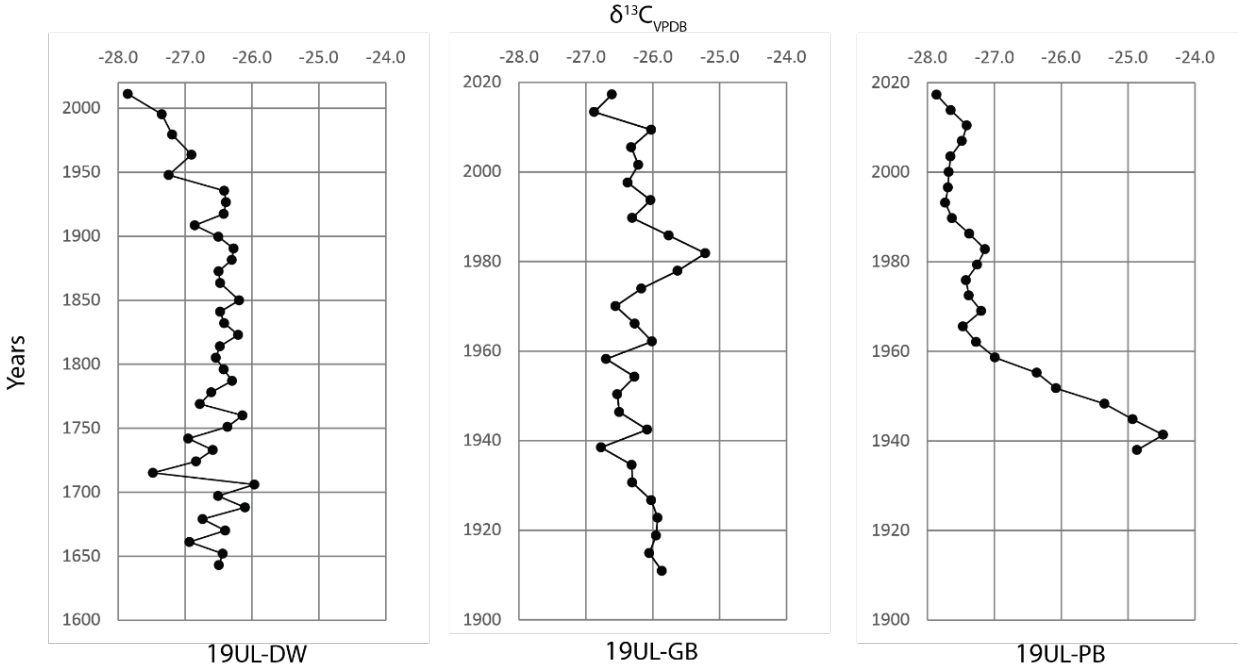

Figure 10. $\delta^{13}C$ values of organic matter in Utah Lake cores. Though all three cores are more negative at the top of the core, 19UL-GB shows an enrichment in values around 1980. These changes in $\delta^{13}C$ values may reflect a change in lake ecology

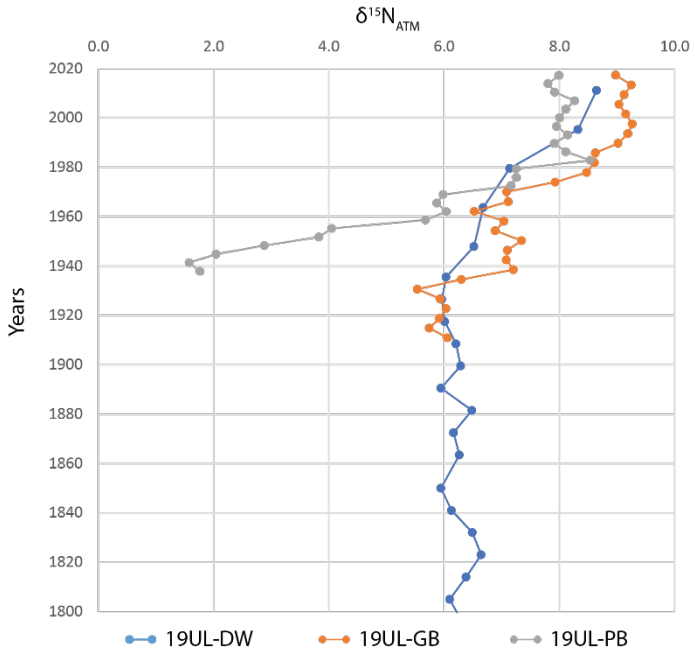

Figure 11. Stacked $\delta^{15}N$ ratio approach similar values towards the top of the cores since 1800. All core values increase between 1930 and 1940. Values at the top of the core range between 8 to 9‰. Values in Provo Bay are lower than both cores until approximately 1960.

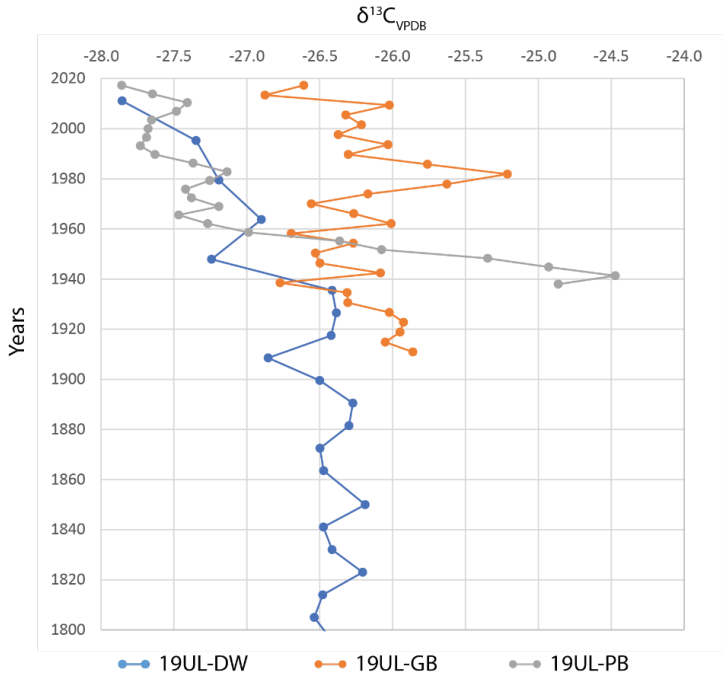

Figure 12. Stacked $\delta^{13}C$ values since 1800. 19UL-DW and 19UL-PB approach similar values towards the top of the core, while 19UL-GB does not start a negative trend until after 1980.

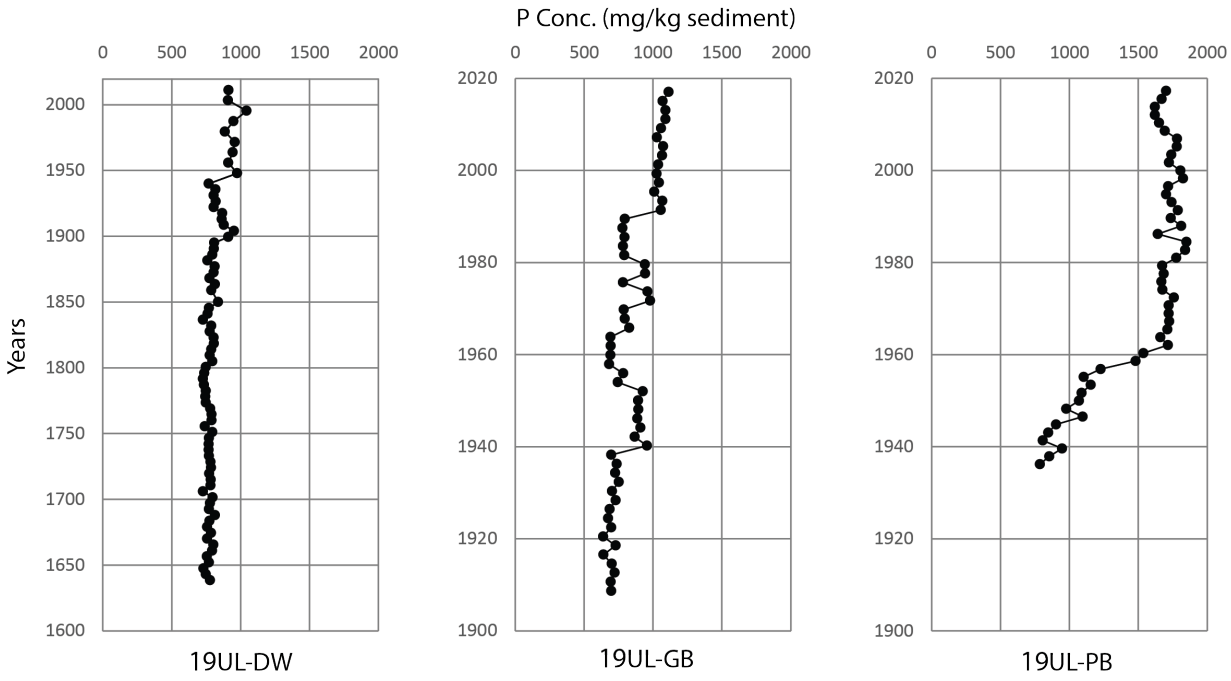

Figure 13. Changing sediment concentrations of P in Utah Lake Cores. All three cores rise in concentrations though 19UL-DW begins rising in the late 1800s, which may represent anthropogenic loading from early settlements. 19UL-GB and 19UL-PB begin to rise in the 1940s, which represent more anthropogenic input as populations rose during the late 1940s (US Census, 2019).

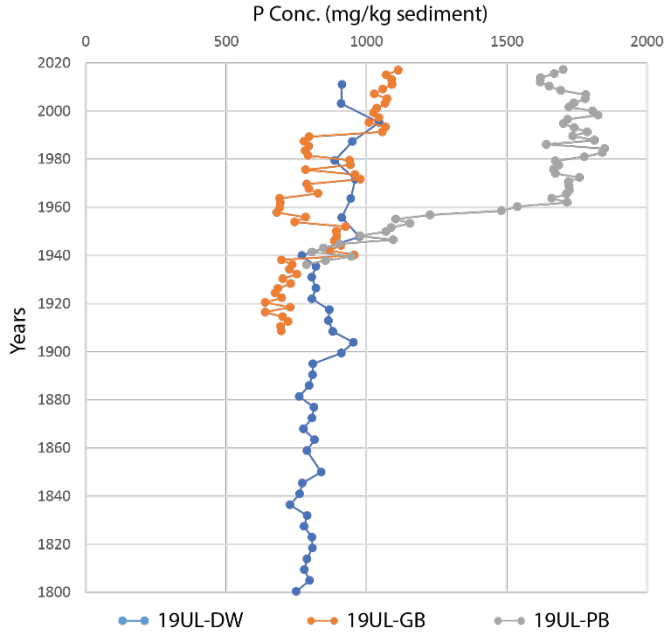

Figure 14. Stacked P concentrations since 1800. 19UL-DW and 19UL-GB show similar concentrations towards the top of the core. 19UL-PB shows the most enrichment and the highest P concentration values. These raised values may be related to anthropogenically influenced discharge, such as storm water runoff and the nearby construction of the Provo WWTP, which discharges into the bay.

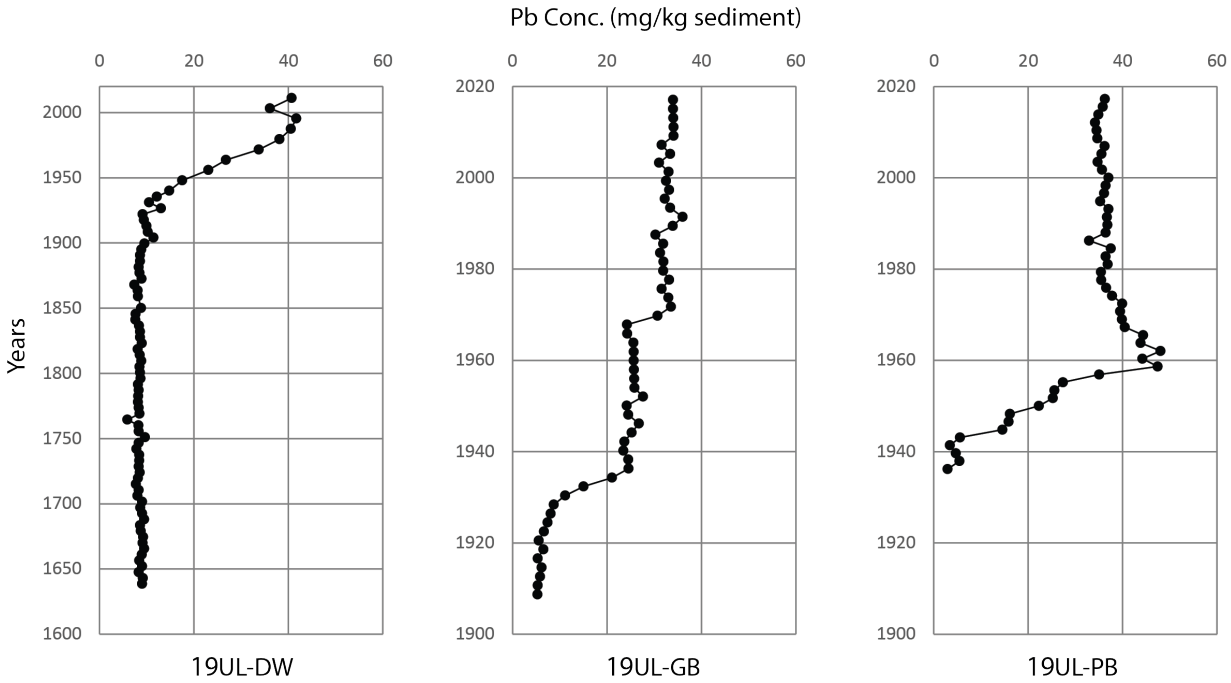

Figure 15. Pb concentrations in Utah Lake cores. All three cores begin to have elevated concentrations of Pb between 1920 and 1950. The increase in Pb concentrations may represent more industrial effluent being loaded into the lake from steel and iron mills.

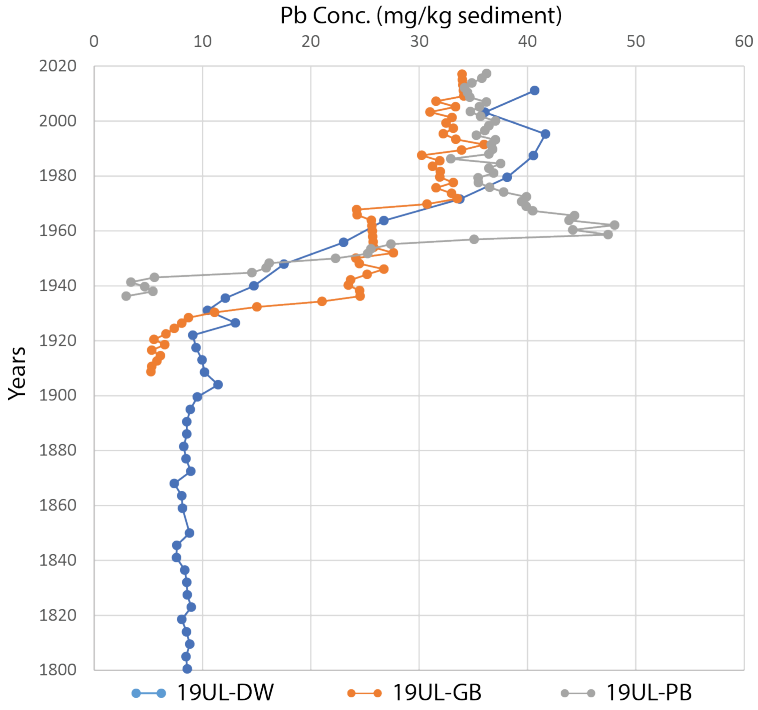

Figure 16. Stacked Pb concentrations after 1800. All three cores reach similar Pb concentrations around 1980s.

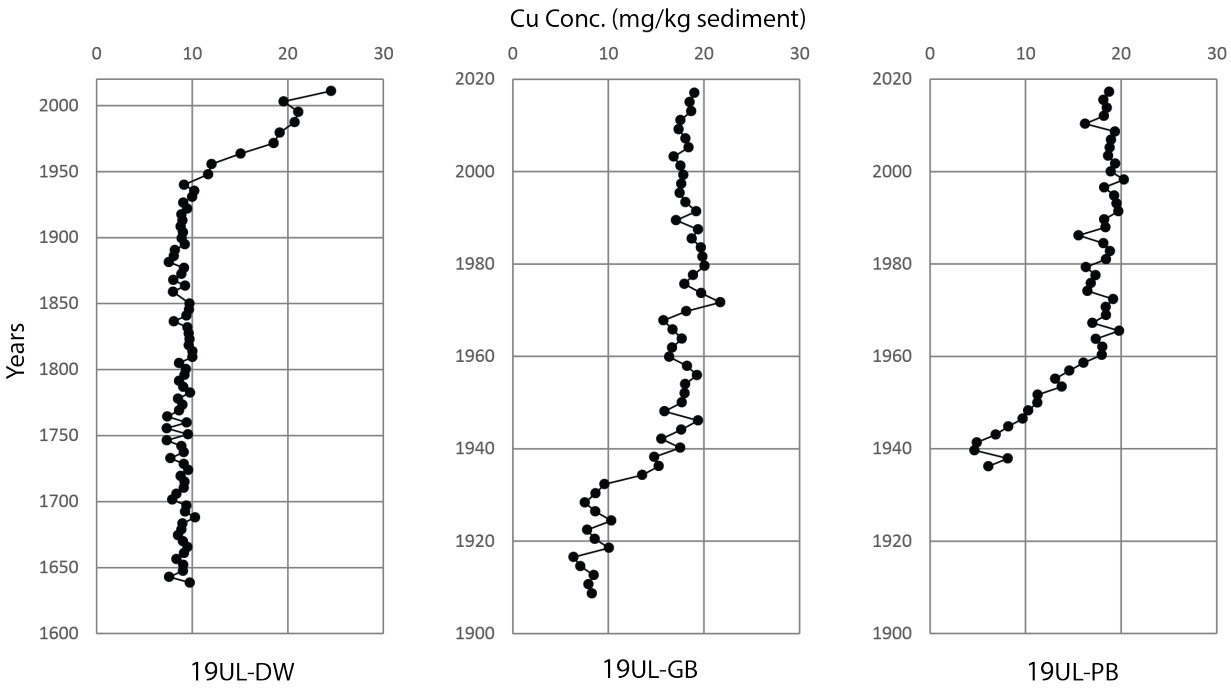

Figure 17. Cu concentrations in Utah Lake cores. Similar to Pb analyses, all three cores have elevated concentrations of Cu between 1920 and 1950. The increase in Cu concentrations may also represent more nutrients from industrial effluent

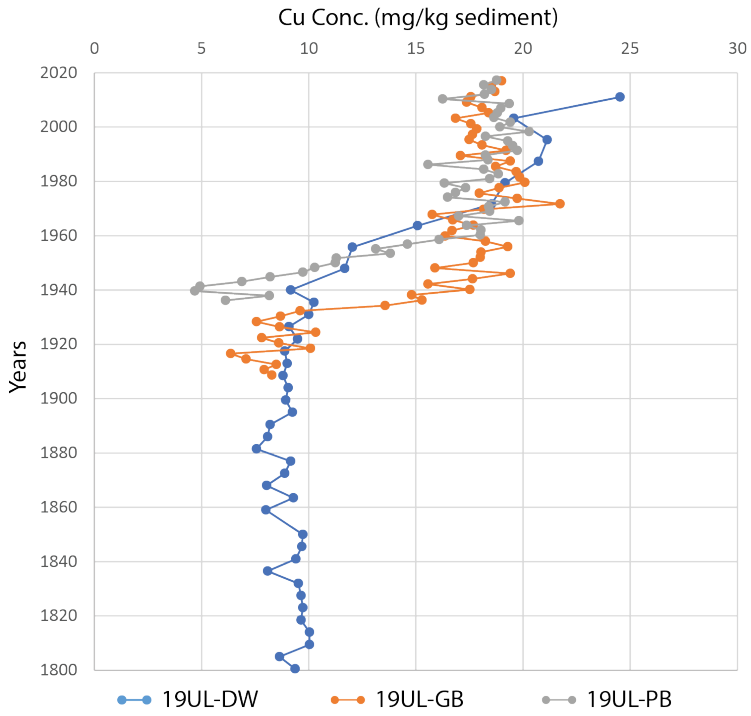

Figure 18. Stacked Cu concentrations after 1800. Similar to Pb analyses, all three cores reach similar elevated values around 1960, though 19UL-DW continues to increase after 2000. This increase may be related to the core being closer to runoff from Geneva Steel than the previous two cores.

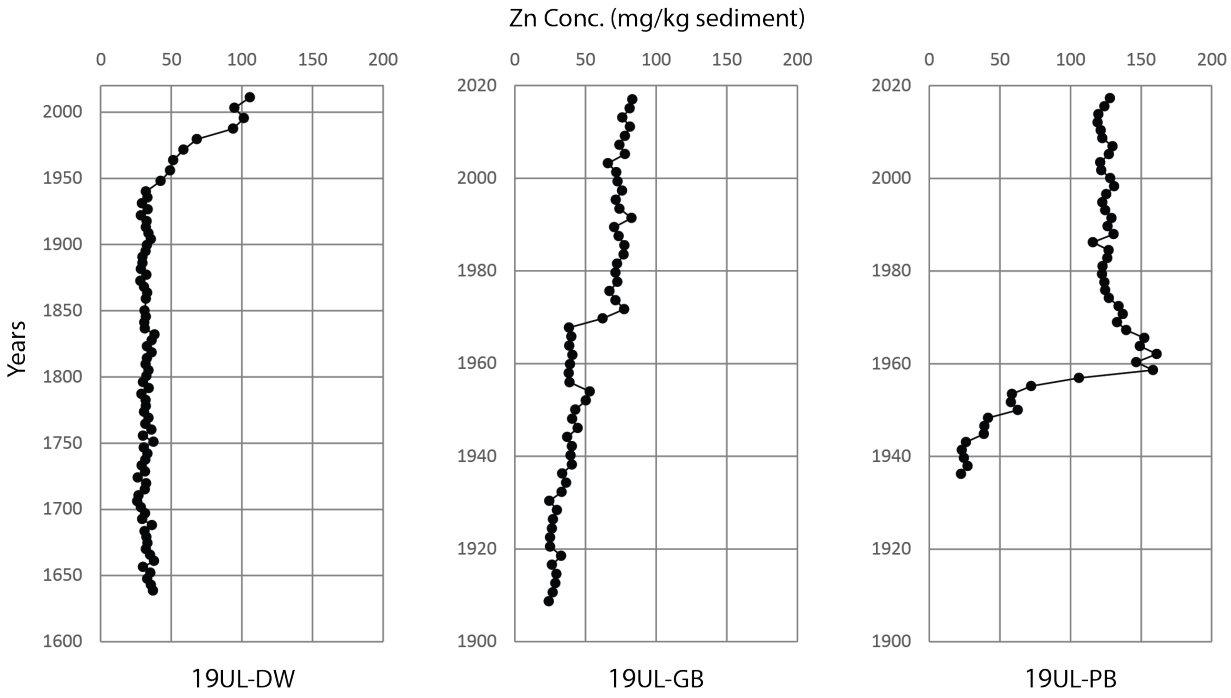

Figure 19. Zn concentration in Utah Lake cores. Zn concentrations also begin rising post-1930s, which corresponds with increased industrial activity in nearby urban areas.

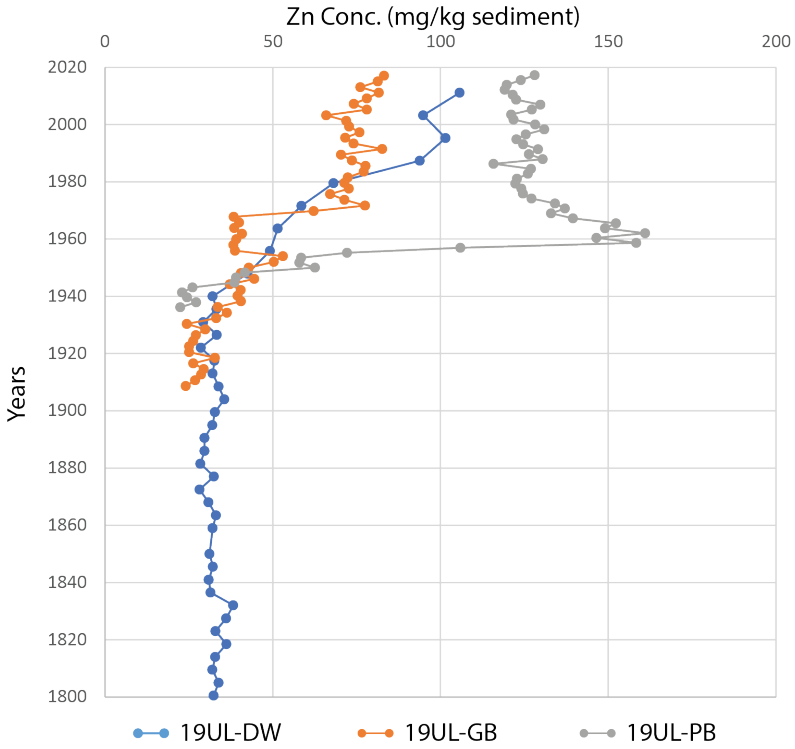

Figure 20. Stacked Zn concentrations after 1800. Lower Zn values in 19UL-GB may be due to less influence from anthropogenic discharge as it is furthest away from concentrated population centers. Higher concentrations in 19UL-PB may be due to more anthropogenic discharge which may be derived from the nearby industry, storm water runoff and Provo WWTP.

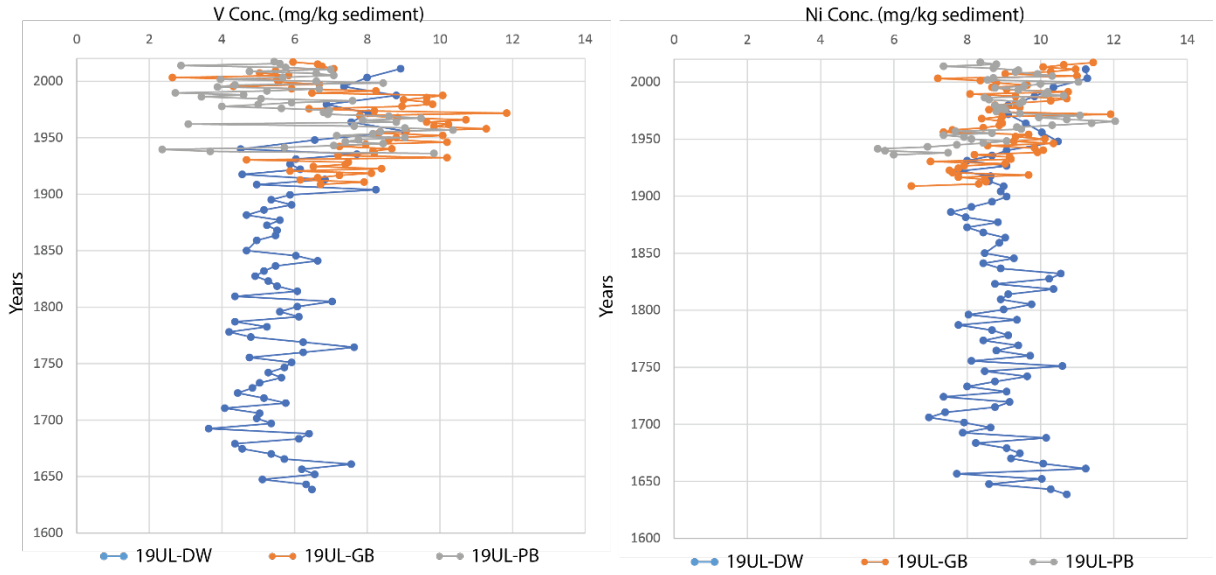

Figure 21. Stacked V and Ni concentrations in Utah Lake cores. Both V and Ni are sensitive to redox conditions and can be used as oxidation indicators. Though both V and Ni values do show some changes in concentration towards the top of the core, which may be from local steel production, the concentrations are low. The low concentration suggests no changes in oxidation states in lake through time.

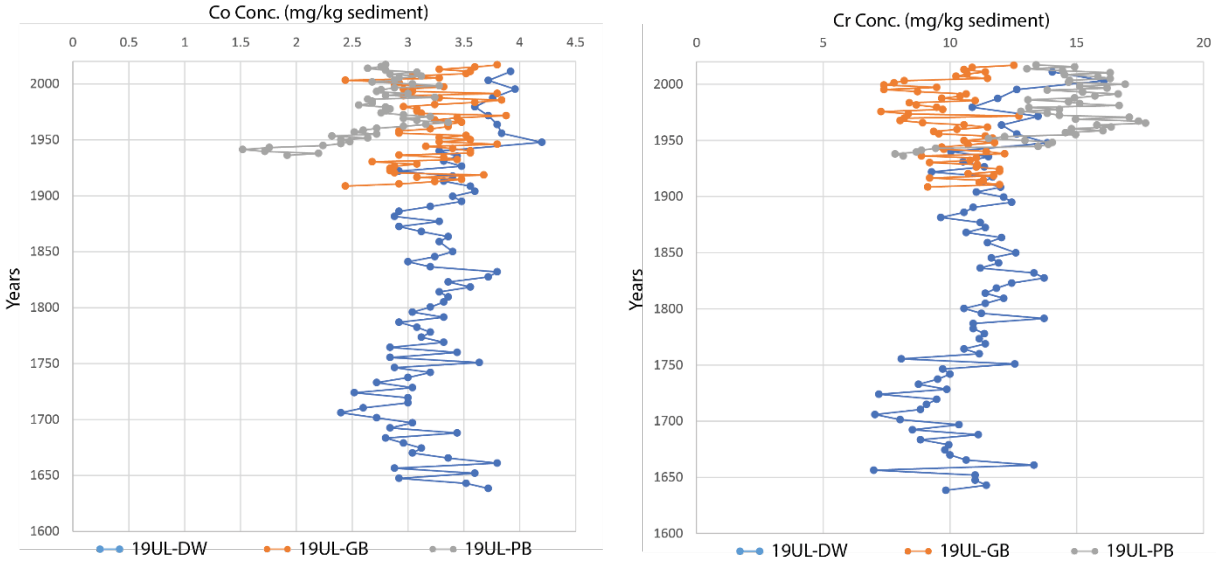

Figure 22. Stacked Co and Cr concentrations in Utah Lake cores. Cores 19UL-DW and 19UL-PB show enrichment in Co and Cr concentrations which may be from industrial effluent. 19UL-GB shows no easily discernable trends in Co and Cr concentrations which may be due to its increased distance from industrial centers compared to the other two cores.

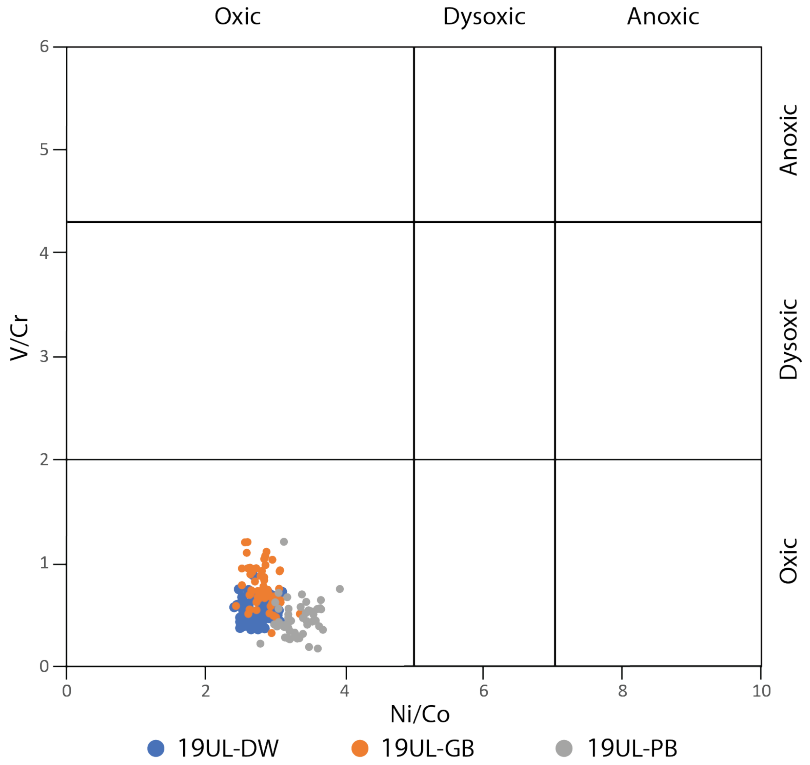

Figure 23. Redox States of Utah Lake Cores samples. Note that all three cores plot well within the oxic range, suggesting that the lake is well-mixed. The anoxic conditions that may be caused by the increased eutrophication-driven primary production may be insignificant when compared to oxic conditions of the lake caused by wave action and mixing.

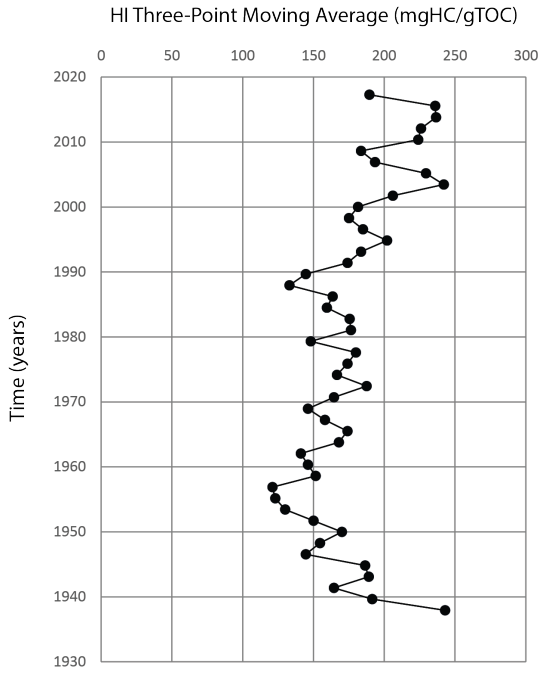

Figure 24. Three-point Moving Average of HI values in 19UL-PB. Notice how the positive deflection to higher HI values is clearer and begins to rise around 1955.

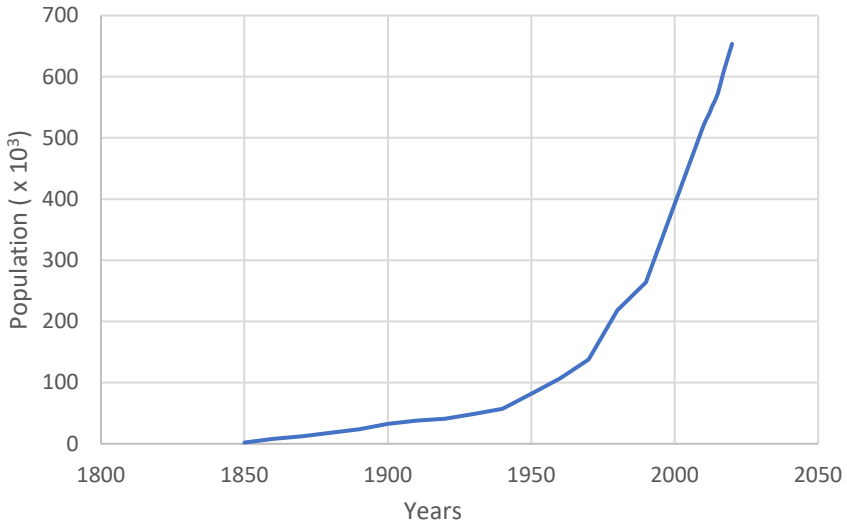

Figure 25. Population of Utah Valley, Utah since 1850. The most rapid population growth occurs after 1950, right after the construction of Geneva Steel (US Census, 2019).

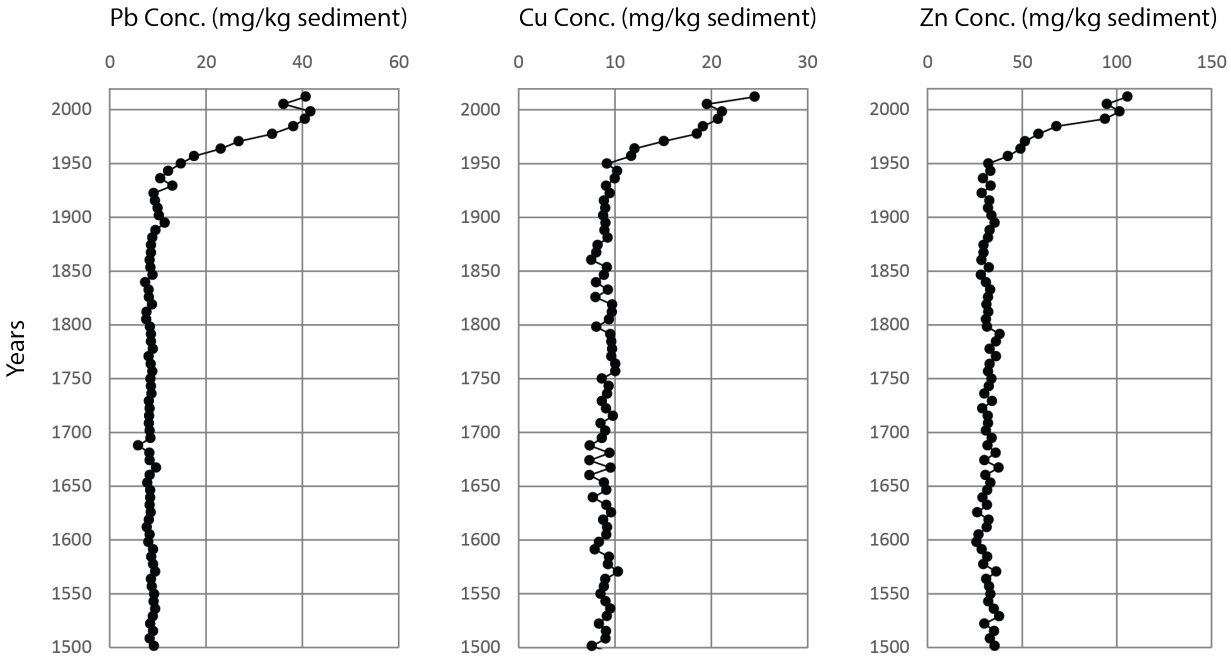

Figure 26. Trace Metal concentrations in 19UL-DW. Note how all trace metals concentrations begin to rise post-1950s. The rise in concentrations may represent Utah Lake being affected by the construction of Geneva Steel.

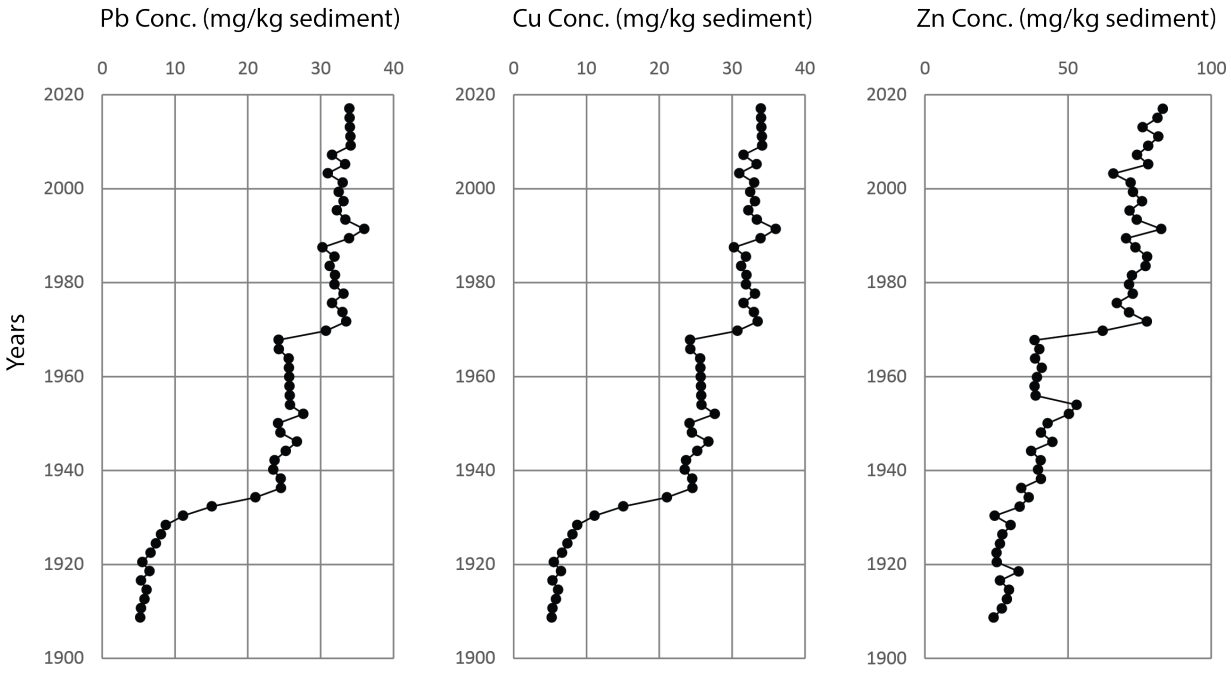

Figure 27. Trace Metal concentrations in 19UL-GB. Trace metals concentrations begin to rise late 1920s. The first rise (late 1920s) in concentrations may represent Utah Lake being affected by the construction of the Tintic Reduction Standard Mill, on the south side of Goshen Bay, and the Columbia Ironton Plant. The second shift may represent where Goshen Bay is being influenced from effluent from Geneva Steel.

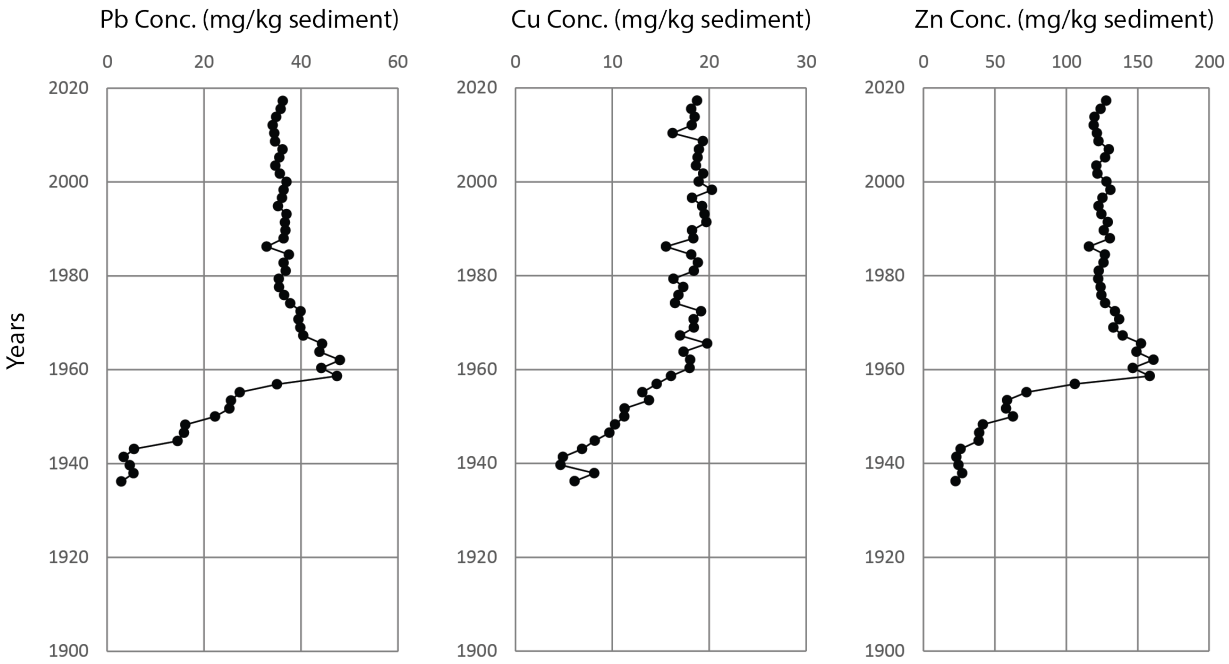

Figure 28. Trace Metal concentrations in 19UL-PB. Trace metals concentrations are already rising pre-1940s. This may represent the lake being affected by the construction of the Columbia Ironton Plant, which was constructed just east of Provo Bay.

8.0 References

Appleby P. G., (2002) Chronostratigraphic Techniques in Recent Sediments, In: W.M., Smol J.P., (eds) *Tracking Environmental Change Using Lake Sediments*, vol 1. Springer, Dordrecht

Aravena R., Evans, M. L., Cherry, J. A., (1993) Stable Isotopes of Oxygen and Nitrogen in Source Identification from Septic Systems. *Groundwater 31* (2) 180-186. doi:10.1111/j.1745-6584.1993.tb01809.x

Baudin, F., Disnar, J., Aboussou, A., Savignac, F., (2015) Guidelines for Rock-Eval analysis of recent marine sediments. *Organic Geochemistry. 86* ( ) 71-80. doi:10.1016/j.orggeochem.2015.06.009

Bish, D. L., Post, J. E., (1993) Quantitative mineralogical analysis using the Rietveld full-pattern fitting method. *American Mineralogist. 78* (9-10) 932-940.

Bradshaw, J.S., Sundrud, R.B., Barton, J.R., Fuhriman, D.K., Loveridge, E.L., Pratt, D.R., (1976). Chemical Response of Utah Lake to Nutrient Inflow, *Water Pollution Control Federation*. *45* (5) 880-887. Retrieved July 9, 2021, from http://www.jstor.org/stable/25037836

Brenner, M., Whitmore, T., Curtis, J., Hodell, D., Schelske, C., (1999). Stable isotope (13C and 15N) signatures of sedimented organic matter as indicators of historic lake trophic state. *Journal of Paleolimnology*. *22*(205-221). doi:10.1023/A:1008078222806.

Biek, R., Geologic map of the Lehi quadrangle and part of the Timpanogos quadrangle, Salt Lake and Utah Counties, Utah. M-210. *Utah Geological Survey.* 1:24,000 scale

Brimhall, W. H., Merritt, L. B., (1981) Geology of Utah Lake: implications for resource management. *Great Basin Naturalist Memoirs. 5.* Utah Lake Monographs, Article 3

Burford, M. A., Carey, C. C., Hamilton, D. P., Huisman, J., Paerl, H. W., Wood, S. A., Wulff, A., (2020) Perspective: Advancing the research agenda for improving understanding of cyanobacteria in a future of global change. *Harmful Algae. 9.* doi:10.1016/j.hal.2019.04.004

Chambers, R.M., Meyerson, L.A., Saltonstall, K., (1999). Expansion of Phragmites australis into wetlands of North America. *Aquatic Botany*. *64* (3-4) 261-273. 10.1016/S0304-3770(99)00055-8.

Chatterjee, M., Silva Filho, E. V., Sarkar, S. K., Sella, S. M., Bhattacharya, A., Satpathy, K. K., Prasad, M. V. R., Chakraborty, S., Battacharya, B. D., (2007). Distribution and possible source of trace elements in the sediment cores of a tropical macrotidal estuary and their

ecotoxicological significance. *Environment International, 33* (3) 346-356. doi:10.1016/j.envint.2006.11.013

Chislock, M. F., Doster, E., Zitomer, R. A., Wilson, A. E., (2013) Eutrophication: Causes, Consequences, and Controls in Aquatic Ecosystems. *Nature Education Knowledge*. *4* (4)10

Choi, W., Ro, H., Chang, S. X., (2005) Carbon isotope composition of Phragmites *australis* in a constructed saline wetland. *Aquatic Botany. 82* (1) 27-38. doi:10.1016/j.aquabot.2005.02.005

Clark, I. D., Fritz, P. (1997). *Environmental Isotopes in Hydrogeology*. Lewis.

Clark, D. L., (2009) Geologic map of the West Mountain quadrangle, Utah County, Utah. M-234. Utah Geological Survey 1:24,000 scale

Constenius, K. N., Clark, D. L., King, J. K., Ehler, J. B., (2011) Interim Geologic Map of the Provo 30' X 60' Quadrangle, Utah, Wasatch and Salt Lake Counties, Utah. *Open-File Report.* Utah Geological Survey

Dickinson, W. R., (2006) Geotectonic evolution of the Great Basin. *Geosphere. 2* (7) 353-368 doi:10.1130/GES00054.1

Dusini, D. S., Foster, D. L., Shore, J. A., Merry, C., (2009) The effect of Lake Erie water level variations on sediment resuspension. *Journal of Great Lakes Research. 35* (1) 1-12. doi:10.1016/j.jglr.2008.04.001

Faegri, K., Iversen, J., (1989) Textbook of Pollen Analysis, 4th ed. John Wiley & Sons, Chichester, UK.

Gichuki, J., Treist, L., Dehairs, F., (2001) The use of stable carbon isotopes as tracers of ecosystem in functioning wetland ecosystems of Lake Victoria, Kenya. *Hydrobiologia. 458* ( ) 91-97. doi:10.1023/A:1013188229590

Gilbert, P. M., Berdalet, E., Burford, M., Pitcher, G., Zhou, M., (2018) Key Questions and Recent Research Advances on Harmful Algal Blooms in Relation to Nutrients and Eutrophication. *Ecological Studies (Analysis and Synthesis). 232.* doi:10.1007/978-3-319-70069-4_12

Goslar, T., Ralska-Jasiewiczowa, M., van Geel, B., Łącka, B., Szeroczyńska, K., Chróst, L., Walanus, A., (1999) Anthropogenic changes in the sediment composition of Lake Gośiąż (central Poland), during the last 330 years. *Journal of Paleolimnology. 22* ( ) 171-185. doi:10.1023/A:1008096032117

Gnecco, I., Berretta, C., Lanza, L. G., La Barbera, P., (2005) Storm water pollution in the urban environment of Genoa, Italy. *Atmospheric Research 77* (1-4) 60-73. doi:10.1016/j.atmosres.2004.10.017

Heath, C. R., Leadbeater, B. C. S., Callow, M. E., (1995) Effect of inhibitors on calcium carbonate deposition mediated by freshwater algae. *Journal of Applied Phycology. 7* ( ) 367-380

Hein, J. R., Perkins, R. B., McIntyre, B. R., (2004) Chapter 2 Evolution of thought concerning the origin of the Phosphoria Formation, Western US Phosphate Fields, *Handbook of Exploration and Environmental Geochemistry 8* ( ) 19-42. Elsevier Science B.V. doi:10.1016/S1874-2734(04)80004-4

Hidden Waters, Jordan and Salt Lake Canal, (na), retrieved from https//hiddenwater.org/saltLakeCanal , J. Willard Marriot Library, University of Utah

Hope B. K., (1997) An assessment of the global impact of anthropogenic vanadium. *Biogeochemistry 37*( ) 1-13.

Horns, D., (2005) Utah Lake Comprehensive Management Plan: Resource Document, *Fires and State Land.* Utah Department of Forestry

Huang J., Huang F., Evans, L., Glasauer, S., (2015) Vanadium: Global (bio)geochemistry. *Chemical Geology 417*( ) 68-89 doi:10.1016/j.chemgeo.2015.09.019

James L.P., (1984). The Tintic Mining District. *Survey Notes*. *18*(2). Utah Geological and Mineral Survey

Jarvie, H.P., Neal, C., Withers, P., (2006). Sewage-effluent phosphorus: A greater risk to river eutrophication than agricultural phosphorus?. Science of The Total Environment. 360. (1-3) 246-253. doi:10.1016/j.scitotenv.2005.08.038.

Landsberg J.H., (2002) The Effects of Harmful Algal Blooms on Aquatic Organisms. *Reviews in Fisheries Science. 10* (2) 113-390 doi:10.1080/20026491051695

Legret, M., Pagotto, C., (1999). Evaluation of pollutant loadings in the runoff waters from a major rural highway. *The Science of the Total Environment. 235* (1-3) 143-150. doi:10.1016/S0048-9697(99)00207-7

Machete, M. N., Personius, S. F., Nelson, A. R., Schwartz, D. P., Lund, W. R., (1991) The Wasatch Fault Zone, Utah, segmentation and history of Holocene Earthquakes. *Journal of Structural Geology. 13* (22) 137-149. doi:10.1016/0191-8141(91)900062-N

McGlathery, K. J., Marino, R., Howarth, R. W., (1994) Variable rates of phosphate uptake by shallow marine carbonate sediments: Mechanisms and ecological significance, *Biogeochemistry 25*( ) 127-146 doi:10.1007/BF00000882

Merritt, L. B., Miller, W. A., (2016) Nutrient Loading to Utah Lake. *Utah Lake Studies.* Jordan River, Farmington Bay and Utah Lake Water Quality Council

Moffitt, J.C., (1975). The story of Provo, Utah. *Press Publishing Company*

Nelson, S. T., Harris, R. A., Dorais, M. J., Heizler, M., Constenius, K. N., Barnett, D. E., (2002) Basement complexes in the Wasatch fault, Utah provide new limits on crustal accretion. *Geology. 30* (9) 831-834. doi:10.1130/0091-7613(2002)030<0831:BCITWF>2.0.CO;2

Peters, K. E., (1986) Guidelines for Evaluating Petroleum Source Rock Using Programmed Pyrolysis. *The American Association of Petroleum Geologists Bulletin. 70* (3) 318-329

Petersen, K. L., Mehringer, P. J. Jr., and Gustafson, C. E., 1983, Late-Glacial Vegetation and Climate at the Manis Mastodon Site, Olympic Peninsula, Washington. *Quaternary Research*, *20* () 215-231.

Poznanović Spahić, M. M., Sakan, S. M., Glavaš-Trbić, B. M., Tančić, P. I., Škrivanj, S. B., Kovačević, J. R., Manojlović, D. D., (2019) Natural and anthropogenic sources of chromium, nickel and cobalt in soils impacted by agricultural and industrial activity (Vojvodina, Serbia), *Journal of Environmental Science and Health*, Part A, *54*(3), 219-230, doi: 10.1080/10934529.2018.1544802

PSOMAS, (2007) Utah Lake TMDL: Pollutant Loading Assessment and Designated Beneficial Use Impairment Assessment, Prepared for: State of Utah Division of Water Quality

Randall, M. C., Carling, G. T., Dastrup, D. B., Miller, T., Nelson, S. T., Rey, K. A., Bickmore, B. R., Aanderud, Z. T., (2019) Sediment potentially controls in-lake phosphorous cycling and harmful cyanobacteria in shallow eutrophic Utah Lake. *PLoS ONE.* doi:10.1371/journal.pone.0212238

Rice, K. C., Conko, K. M., Hornberger, G. M., (2002) Anthropogenic Sources of Arsenic and Copper to Sediments in a Suburban Lake, North Virginia. *Environ. Sci. Technol. 36* (23) 4962-4967. doi:10.1021/es025727x

Riquier. L., Tribovillard, N., Averbuch, O., Devleeschouwer, X., Riboulleau, A., (2006) The Late Frasnian Kellwasser horizons of the Harz Mountains (Germany): Two oxygen-deficient periods resulting from different mechanisms, *Chemical Geology 233*( ) 137-155 doi:10.1016/jchemgeo.2006.02.021

Romano, E., Bergamin, L., Magno, M.C., Pierfranceschi G., Ausili, A., (2018). Temporal changes of metal and trace element contamination in marine sediments due to a steel plant: The case study of Bagnoli (Naples, Italy). *Applied Geochemistry 88* (A) 10.1016/j.apgeochem.2017.05.012.

Roper, R. (1994). *GENEVA STEEL PLANT*. Utah History Encyclopedia. https://www.uen.org/utah_history_encyclopedia/g/GENEVA_STEEL.shtml.

Seyferth D., (2003). The Rise and Fall of Tetraethyllead. 2. *Organometallics*. *22* (25). 10.1021/om030621b, American Chemical Society

Shaw, B. H., Mechenich, C., Klessig, L. L., (2004) Understanding Lake Data, Board of Regents of the University of Wisconsin System

Smith, J.N., Lee, K., Gobeil, C., Macdonald, R.W., (2008). Natural rates of sediment containment of PAH, PCB and metal inventories in Sydney Harbour, Nova Scotia. *Science of the Total Environment*. *407*(17) 4858-4869. doi:10.1016/j.scitotenv.2009.05.029.

Smith, V. H., Schindler, D. W., (2009) Eutrophication science: Where do we go from here?. *Trends in Ecology and Evolution. 24*(4) 201-207.

Siver, P.A., Wozniak, J.A., (2001) Lead analysis of sediment cores from seven Connecticut lakes, *Journal of Paleolimnology*. *26* (1-10). Kluwer Academic Publishers. doi:10.1023/A:1011131201092

Solomon, B. J., (2010) Interim Geologic Map of unconsolidated deposits in the Santaquin quadrangle, Utah and Juab counties, Utah. *Open-File Report 570.* Utah Geological Survey

Spangler, D. K., (2019) Algal Blooms Abound: Permanent Signs Tell About Risks. *Utah Department of Environmental Quality.* https://deq.utah.gov/communication/news/algal-blooms-abound-permanent-sings-tell-about-risks

Strong, A. E., (1974) Remote Sensing of Algal Blooms by Aircraft and Satellite in Lake Erie and Utah Lake, *Remote Sensing of the Environment. 3,* (2) 99-107 doi:10.1016/0034-4257(74)90052-2

Talbot, M. R., Lærdal, T., (2000) The Late Pleistocene – Holocene palaeolimnology of Lake Victoria, East Africa, based on elemental and isotopic analyses of sedimentary organic matter. *Journal of Paleolimnology*. *23* ( ) 141-164. doi:10.1023/A:1008029400463

Talbot M.R., Livingstone D.A., (1989) Hydrogen index and carbon isotopes of lacustrine organic matter as lake level indicators. *Paleogeography, Paleoclimatology, Paleoecology. 70* ( ) 121-137

Tong, S. T. Y., Naramngam, S., (2007) Modeling the Impacts of Farming Practices on Water Quality in the Little Miami River Basin, *Environ Manage. 39* ( ) 853-866. doi:10.1007/s00267-006-0307-6

US Census Bureau. (2019) *QuickFacts Utah; Utah County, Utah*. United States Census Bureau. https://www.census.gov/quickfacts/fact/table/utahcountyutah/PST045219#PST045219.

Utah Division of Water Resources, (2010) Jordan River Basin; Planning for the Future. *Utah State Water Plan.* www.water.utah.gov

Wada E., (2009) Stable δ15N and δ13C isotope ratios in aquatic ecosystems. *Proceedings of the Japan Academy*, Series B Physical and Biological Sciences, pp 90-107

Wang, C., Hu, X., Chen, M., Wu, Y., (2005) Total concentrations and fractions of Cd, Cr, Pb, Cu, Ni, and Zn in sewage sludge from municipal and industrial wastewater treatment plants, *Journal of Hazardous Materials. 119* (1-3) 245 – 249 doi:10.1016/j.jhazmat.2004.11.023

Widory, D., Kloppmann, W., Chery, L., Bonnin, J., Rochdi, H., Guinamant, J., (2004) Nitrate in groundwater: an isotopic multi-tracer approach. *Journal of Contaminant Hydrology. 72* (1-4) 165-188. doi:10.1016/j.jconhyd.2003.10.010

Xiang L., Li Y., Liu B., Zhao H., Li H., Cai Q., Mo C., Wong M., Li Q. X., (2019) High ecological and human health risks from microsystins in vegetable fields in southern China: *Environmental International*. *133* (A) 105-142 doi:10.1016/j.envint.2019.105142

Yang, H., Linge, K., Rose, N., (2007) The Pb pollution fingerprint at Lochnagar: The historical record and current status of Pb isotopes. *Environmental Pollution. 145* (3) 723-729. doi:10.1016/j.envpol.2006.06.026

Zamora-Barrios C. A., Nandini S., Sarma S. S. S., (2019) Bioaccumulation of microsystins in seston, zooplankton and fish: A case study in Lake Zumpango, Mexico. *Environmental Pollution*. *249* ( ) 267-276. doi:10.1016/j.envpol.2019.03.029

Zanchett, G., Oliveria-Filho, E. C., (2013) Cyanobacteria and Cyanotoxins: From Impacts on Aquatic Ecosystems and Human Health to Anticarcinogenic Effects. *Toxins. 5* (10) 1896-1917. doi:10.3390/toxins5101896

Zhang, L., Du, Y., Du, C., Xu, M., Loaiciga, H. A., (2016) The adsorption/desorption of phosphorus in freshwater sediments from buffer zones: the effects of sediment concentration and pH, *Environ Monit Assess. 188* (13). doi:10.1007/s10661-015-5018-0

Zhu G., Wang F., Zhang Y., Gao G., Qin B., (2008) Hypoxia and its environmental influences in large, shallow, and eutrophic Lake Taihu, China; *Internationale Vereinigung für theoretische und angewandte Limnologie: Verhandlungen*. *30* (3) 361-365. doi:10.1080/03680770.2008.11902144